BULLETIN NO. 36
MARCH 1955

ENGINEERING EXPERIMENT STATION
OREGON STATE COLLEGE
CORVALLIS, OREGON

A STUDY OF DUCTILE IRON AND ITS RESPONSE TO WELDING

By

W. H. RICE
Associate Professor
Welding
Oklahoma A & M College

O. G. PAASCHE
Associate Professor
Mechanical Engineering
Oregon State College

THE Oregon State Engineering Experiment Station was established by act of the Board of Regents of Oregon State College on May 4, 1927. It is the purpose of the Station to serve the state in a manner broadly outlined by the following policy:

(1) To stimulate and elevate engineering education by developing the research spirit in faculty and students.

(2) To serve the industries, utilities, professional engineers, public departments, and engineering teachers by making investigations of interest to them.

(3) To publish and distribute by bulletins, circulars, and technical articles in periodicals the results of such studies, surveys, tests, investigations, and research as will be of greatest benefit to the people of Oregon, and particularly to the state's industries, utilities, and professional engineers.

To make available the results of the investigations conducted by the Station, three types of publications are issued. These are:

(1) *Bulletins* covering original investigations.

(2) *Circulars* giving compilations of useful data.

(3) *Reprints* giving more general distribution to scientific papers or reports previously published elsewhere, as for example, in the proceedings of professional societies.

Single copies of publications are sent free on request to residents of Oregon, to libraries, and to other experiment stations exchanging publications. As long as available, additional copies, or copies to others, are sent at prices covering cost of printing. The price of this publication is 60 cents.

For copies of publications or for other information address:

Oregon State Engineering Experiment Station,

Corvallis, Oregon

A STUDY OF DUCTILE IRON AND ITS RESPONSE TO WELDING

by

W. H. RICE

Associate Professor of Welding
Oklahoma A & M College

and

O. G. PAASCHE

Associate Professor of Mechanical Engineering
Oregon State College

BULLETIN NO. 36

MARCH 1955

Engineering Experiment Station
Oregon State System of Higher Education
Oregon State College
Corvallis

Foreword and Acknowledgments

The information presented in this bulletin is the result of an Engineering Experiment Station project. The investigation was made under the direction of Professor S. H. Graf, former director of the Engineering Experiment Station, and his successor, Professor Milosh Popovich.

All castings used during the study were provided without charge by the Holt Equipment Company of Independence, Oregon, and the Eagle Foundry Company of Seattle, Washington. The cooperation and assistance of Mr. Douglas Blair and Mr. E. M. Uebel of these respective companies are particularly appreciated.

Advice and assistance in many forms were freely given by numerous faculty members and other individuals. Appreciation is especially expressed to Professors James W. Smith and Asa A. Robley of the Industrial Arts Department at Oregon State College and to Albert G. Zima, head of the West Coast Technical Section of the International Nickel Company, Los Angeles, California.

The assistance of several engineering students in preparing test specimens and in conducting tests and metallographic examination is also gratefully acknowledged. These students include Donald H. West, Charles R. Utterback, Richard F. Stevens, and B. M. Darrow.

Table of Contents

Table of Contents—(Cont'd)

Illustrations

Tables

A Study of Ductile Iron and Its Response to Welding

by
W. H. Rice
and
O. G. Paasche

Summary

Ductile or nodular cast iron developed by the International Nickel Company, provides the strength and ductility of steel together with the competitive cost of gray cast iron. Countless industrial applications have been found for this material since its initial production in 1948. Very little information has been available to date in regard to methods of welding and the physical properties that can be expected for ductile iron which would enable the designer to freely specify this method of fabrication.

The welding methods investigated included the metallic arc with Ni-Rod 55, E6013 mild steel, E6015 low hydrogen, 18 Cr-8 Ni stainless steel, and 25 Cr-20 Ni stainless-steel electrodes, as well as the carbon arc, inert gas-shielded arc, and oxyacetylene fusion welding and brazing. The effects of welding in both the as-cast and annealed conditions were observed, together with the benefits of preheating and post-welding annealing.

The best physical properties were obtained by carbon-arc welding, which also provided a rapid deposition rate and ease of application. This method would be excellent for salvage of defective castings or for repair of broken castings. If high preheating and postheating are not desired, Ni-Rod 55 would be the best electrode choice. The best electrode choice for welding ductile iron to steel or other metals is Ni-Rod 55.

If the fabricator is insistent upon an inexpensive steel electrode, the low hydrogen E6015 or E6016 types are recommended, although they provide somewhat lower physical properties than Ni-Rod 55. In using these electrodes, some fusion-line cracking is encountered with high silicon iron, and their normal tendency toward producing brittle joints is increased, with iron having a phosphorus content of over 0.05%. Severe underbead cracking is encountered with mild-steel electrodes other than the low-hydrogen type, and it is recommended their use be avoided.

I. Introduction

1. **Introductory comment.** Ductile iron is a cast, ferrous product quite similar to gray cast iron in composition yet possessing the strength and ductility of steel. This material, developed by the International Nickel Company at Bayonne, New Jersey, in 1948, has received wide acclaim as being one of the most important engineering materials developed in recent years.

2. **Origin and properties of gray iron.** Although cast iron was utilized by the Chinese prior to the time of Christ, it was not known to the western civilized world until its discovery early in the 14th century, when it was first used in Germany for cannon and other implements of war. Since that time greater tonnages of gray cast iron have been produced in cast form than of all other metals combined. In the present day it is not only widely used throughout all industry, but is also found in many forms in every household and on every farm.

Gray cast iron is regarded by the metallurgist as an iron-base alloy with 2.0 to 4.0% carbon. It has a steel matrix which contains from 0.10 to 0.90% carbon in the form of cementite or iron carbide, with remaining carbon in the form of flake graphite. The tensile strength of gray iron, which ranges from 20,000 to 60,000 psi, is far less than that of steel with a similar matrix. The weakness is attributed to interference with grain structure by the presence of graphite in flake form.

3. **Development of nodular iron.** Metallurgists have been aware for a long time that free carbon in cast iron, if made to form into nodules instead of flakes, would vastly improve mechanical properties of the material by eliminating the internal notching effect of the graphite flakes and decreasing surface area of the free carbon.

International Nickel Company's discovery resulted in a method of making free carbon form into spheroids in cast iron by means of a ladle addition of a small amount of magnesium. It is believed very minute particles of magnesium oxide act as nuclei of crystallization for free carbon, causing it to form as hexagonal crystalline spheriods. As a result, a material of great economic importance was produced, combining the strength and ductility of cast steel with the reduced cost, wear resistance, and damping characteristics of cast iron. This material, ductile cast iron, is also known as nodular or spheroidal iron.

4. **Nature of the study.** One of the foremost problems concerning this new engineering material was its integration with steel

or other alloys into machinery construction by means of welding. Other problems consisted of the production of built-up castings from simply cast component parts which would be difficult, or perhaps impossible to cast as a whole, and the repair of broken castings or of foundry defects by means of welding.

The problems of welding ductile iron are quite complex. It is actually a family of materials rather than a single material. Its nodules of graphite can exist in ferritic, pearlitic, austenitic, martensitic, or acicularic matrixes, depending upon heat treatment and composition. The heat of welding causes a rapid diffusion of carbon from the nodule into the surrounding steel matrix, where it remains because of the chilling effect of heat transfer by the base metal. All possible structures found in high-carbon and low-alloy steels exist simultaneously with the nodules of graphite. The problems of welding ductile iron are beset, therefore, with the combined difficulties of welding both alloy steel and cast iron.

This investigation was initiated because of the scarcity of information concerning the welding of ductile iron. Only one article had been published on this subject. Little information was available to an engineer for incorporating ductile iron into welded designs, or knowledge concerning industrial repairs of the material.

The continued increase in production of ductile iron, and its constantly improving status as an economic engineering material, has rendered mandatory its integration into fabrication by welding. There is, therefore, an urgent demand on the part of the engineer for specific information on this subject which will assist in practical application of design.

Since inauguration of this study at Oregon State College, four articles have been published elsewhere concerning welding of ductile iron. This would indicate at least four other groups are participating actively in work of this general nature, testimony of the increasing importance of the problem.

The area embraced by the scope of this work is indeed large and much work remains to be accomplished. Although the primary nature of the investigation conducted by each group is different, the combined results fit into a broad pattern. Fortunately, there is sufficient correlation between research programs here and elsewhere, notwithstanding the variance in objectives, that some verification of results can be established.

II. Composition of Ductile Iron

1. **Effect of composition on properties.** One of the primary considerations of ductile iron is its composition. Seemingly small changes in composition can result in a wide variation of such properties as strength, structure, shock resistance, machinability, and others. Composition of the base metal is found to have a marked effect upon its response to welding by different processes. Because composition should be taken into account when considering problems of welding, the following discussion is intended to provide specific information in this respect.

2. **Range of composition.** The chemical compositional limits of ductile cast iron are given in Table 1. An essential difference in composition between gray cast iron and ductile iron is the small amount of magnesium or cerium ductile iron contains. Although magnesium is more commonly used, cerium also will cause graphite to form into spheriods rather than into flakes, as in gray cast iron.

Table 1. COMPOSITIONAL RANGE OF DUCTILE IRON

Compositional classifications	Carbon	Silicon	Manganese	Phosphorus (max)	Nickel	Magnesium
	Per cent	*Per cent*	*Per cent*	*Per cent*	*Per cent*	*Per cent*
Broad-range	3.2–4.2	1.00–4.00	0.1–0.8	0.10	0.0–3.5	0.05–0.10
Ferritic high ductility	3.6–4.2	1.25–2.00	0.35	0.08	0.0–1.0	0.05–0.08
Ferritic high strength	3.4–3.8	2.25–3.25	0.35	0.10	0.0–1.0	0.05–0.08
Pearlitic high strength	3.2–3.8	2.25–2.75	0.6–0.8	0.10	1.5–3.5	0.05–0.08

It is to be noted Table 1 does not include the austenitic ductile-iron castings produced for use under conditions of high temperature and corrosion. Problems concerned with welding high chromium-nickel austenitic castings are not necessarily common to those of ferritic-pearlitic structure and, therefore, are not included in the scope of this investigation. It appears probable that in the near future many alloy grades of ductile cast iron will be developed comparable to various grades of alloy steel.

3. **Effect of silicon.** In addition to the magnesium content, both carbon and silicon are slightly higher in ductile iron than in gray iron. The carbon equivalent in ductile iron (carbon plus one-third

silicon) is normally between 4.3 and 4.6%. The silicon content of gray cast iron is limited because of its coarsening effect on flake graphite. On the other hand, no effect of silicon was noted on size or distribution of carbon nodules in castings used in this study, which ranged from 2.63 to over 4.22% silicon.

Table 1 indicated strengthening of ductile iron by a solid solution of silicon in ferrite, accompanied by decreased ductility and impact resistance. Tensile tests of annealed ductile iron, from various heats made during this study, indicated an increase in strength of over 10,000 psi for each additional 1% of silicon content. The increased tensile strength was accompanied by reduced impact resistance. A 1% increase of silicon lowered the impact resistance from 36.3 foot-pounds to 22.1 foot-pounds for 0.394-inch square unnotched bars.

A $\frac{3}{8}$-inch square bar was removed from a $\frac{1}{2}$-inch Y-block having a chemical analysis of 2.70 carbon, 2.98 silicon, 0.02 sulfur, 0.05 phosphorus, and 0.30 manganese. The end of this bar was hand forged at about 1800° F. and then curled while hot, as shown in Figure 1. The center of the bar was then hot twisted at about 1600° F. This was evidence of the good, hot workability of the material.

A bar of similar dimensions containing 4.22 silicon, 0.032 sulfur, 0.048 phosphorus, and 0.39 manganese, could be hot twisted to the same extent as the one in Figure 1, although it proved to be quite hot short when attempts were made to hot forge it. This characteristic was attributed to the increase in silicon content.

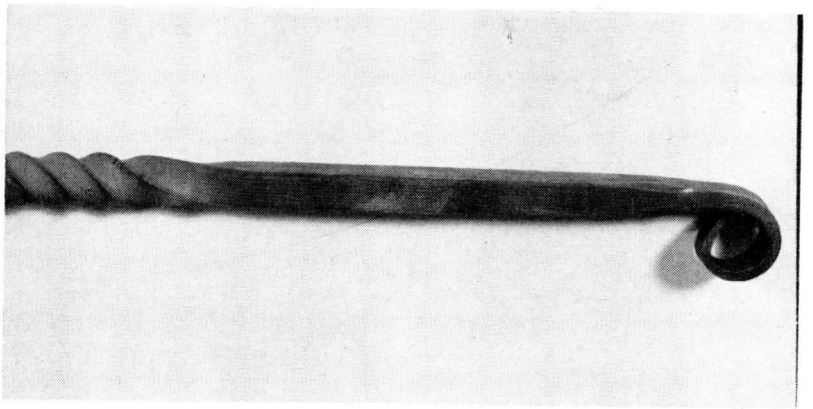

Figure 1. Ductile cast-iron bar that has been forged and hot twisted.

4. **Effect of phosphorus.** Castings obtained during the summer and early fall of 1953 contained less than 0.05% phosphorus,

since Swedish pig iron low in this element was used in the charge. The charge consisted of 10% pig iron and the remainder steel scrap and foundry returns. Later, in the fall of 1953, use of domestically produced pig iron having a high content of phosphorus (0.24%) led to an increased amount of this element in the ductile-iron castings. Foundry returns caused a gradual increase in phosphorus until it was well over the maximum allowable of 0.10%. In late February 1954, it was necessary to lower the bottom of the cupola in order to increase the slag level and to provide more opportunity for removal of phosphorus.

In the basic process, such as that used by the Holt Equipment Company, phosphorus was oxidized, forming P_2O_5 which reacted with the lime slag to form calcium phosphate. The phosphate produced became part of the slag and was poured off.

Annealed castings containing less than 0.05% phosphorus produced an average tensile strength of 66,360 psi with 21.7% elongation. When the phosphorus was increased to 0.086%, with very little change in the remaining composition, strength decreased to 58,900 psi and ductility to 6.62% elongation. This adverse effect on the mechanical properties was attributed to a very fine network of iron-phosphide eutectic and to the tendency of phosphorus to stabilize pearlite.

5. **Composition of material used in study.** Thirty Y-block castings were poured February 25, 1954, which provided test sections $2\frac{1}{2}$ inches wide, $\frac{1}{2}$-inch thick, and 14 inches long. A second heat consisted of 52 castings of similar dimensions which were poured March 4, 1954. The analysis of these two heats are given in Table 2.

Table 2. INFORMATION CONCERNING TWO HEATS OF TEST CASTINGS

Castings	Heat No. 1	Heat No. 2
Composition, per cent		
Magnesium	0.084	0.056
Sulfur	0.018	0.032
Manganese	0.410	0.390
Phosphorus	0.048	0.048
Silicon	3.700	4.220
Nickel	0.740	0.790
Chromium	0.050	0.050
Vanadium	0.120	0.160
Mechanical properties		
Ultimate tensile strength, psi	84,750	88,995
Yield strength at 0.1% offset, psi	71,800	71,505
Elongation in 2 in., per cent	13.0	15.5

Sulfur is always very low in ductile iron and the analysis given in Table 2 is quite typical for this element. In gray cast iron, sulfur increases carbide stability and inhibits graphitization if the manganese content is too low. Manganese forms the relatively insoluble manganese sulphide and manganese silicate existing in the form of less harmful inclusions in the casting. Due to the low sulfur content of ductile iron, the manganese is proportionally lower. If the manganese content of ductile iron is above 0.50%, it stabilizes pearlite to such an extent a completely ferritic structure cannot be obtained by heat treatment.

The chromium and vanadium content in Table 2 does not appear high. These elements are such strong stabilizers that when lower silicon contents are used the amounts indicated are sufficient to cause retention of substantial amounts of massive carbides and fine pearlite, even after annealing 5 hours at 1650° F. followed by cooling at a maximum rate of 40° F./hour from 1500° F., through 1200° F.

Other test castings were samples from numerous heats that represented several months' production. Table 3 is intended to provide information typical of these castings.

Table 3. TYPICAL COMPOSITIONS OF OTHER TEST CASTINGS

Element	1953 Castings		
	September 15	November 3	December 15
Carbon	2.800	2.70	3.200
Silicon	2.910	2.98	2.630
Sulfur	0.017	0.02	0.020
Phosphorus	0.078	0.05	0.086
Manganese	0.380	0.30	.....
Magnesium	0.049	.....	0.067

6. **Carbon equivalent of ductile iron.** It was previously stated the carbon equivalent of ductile iron should be between 4.3 and 4.6%. Carbon equivalents of the typical heats in Table 3 were 3.77, 3.69, and 4.08% respectively. Carbon itself has very little effect upon the mechanical properties of annealed ductile iron. Foundry characteristics such as chilling propensity, feeding requirements, and fluidity were affected, however, and many castings were rejected on the basis of radiographic examination as being unfit for use in this investigation.

As-cast ductility was reduced when the carbon equivalent was low, as evidenced by an average elongation of 1.2% for the castings in Table 3 compared with 3.1% for those in Table 2. It was noted

also that machinability of castings in the as-cast condition in Table 2 was much superior to that of castings in the as-cast condition in Table 3. Lowering the furnace bottom adjusted the carbon equivalent to its proper condition in addition to reducing the phosphorus content, as previously mentioned.

III. Production of Ductile Iron

1. **Foundry procedure.** Overall foundry procedure is perhaps of equal importance to composition if a satisfactory quality of ductile iron is to be obtained. After composition has been established by means of the charge, the next consideration is selection of the most suitable foundry technique. Foundry procedure for producing nodular graphite in cast iron normally involves two steps: (1) a ladle addition of magnesium is added in such a manner that a small but effective portion is retained in the iron; (2) inoculating with a strong graphitizing agent, such as ferrosilicon.

2. **Magnesium addition.** The first effect of magnesium addition must be to reduce sulfur content of the iron to 0.02% or less because magnesium cannot be retained in the iron until the sulfur is reduced to this level. Magnesium volatilizes at about 2100° F., therefore a sufficient amount must be added to allow for sulfur removal, volatilization, and oxidation, yet permit retention of 0.045 to 0.10% magnesium in the iron.

Several magnesium alloys are available for nodular iron production, compositions of which are given in Table 4.

Table 4. COMPOSITION OF MAGNESIUM ALLOY

Magnesium alloys	Magnesium	Nickel	Silicon	Copper	Iron
Inco No. 1	15–20	75–80	.....	.....	Balance
Inco No. 2	15–20	40–50	25–30	.....	"
Inco No. 3	15–20	.....	60–65	.....	"
Vanadium No. 12	12	.....	40	16	"
Electro-Met	8	.....	46	.....	"

An exceedingly violent reaction takes place when pure magnesium encounters molten iron. For this reason, an alloy containing not over 20% magnesium is used as an additive. A sheet-iron shield, illustrated in Figure 2, is used by the Holt Equipment Company to surround the ladle during magnesium addition to protect workmen from the violent reaction taking place.

Electro-Met alloy is used by the Holt Equipment Company to provide magnesium addition in the ratio of 14 pounds per 500-pound ladle of molten iron. This 2.8% addition provides a magnesium recovery in the iron of 25 to 40% of the amount added at 2500° F. Foundries that tap cupola iron at higher temperatures are inclined to use Inco No. 1, No. 2, or Vanadium No. 12 because their greater densities provide a higher recovery of magnesium at more elevated temperatures.

The cast iron is first tapped into a holding ladle attached to a scale in order to provide an accurately known weight of molten metal (Figure 2). The magnesium alloy is then placed in a second ladle and the cast iron is poured on top of it to provide bottom introduction of alloys, which prevents undue volatilization of magnesium. An alloy particle size of about $\frac{3}{4}$-inch diameter has been found most suitable for treatment of iron in this amount. For larger ladle additions of 1000 pounds or more, particle size distribution of 1 to 3 inches provides better magnesium recovery.

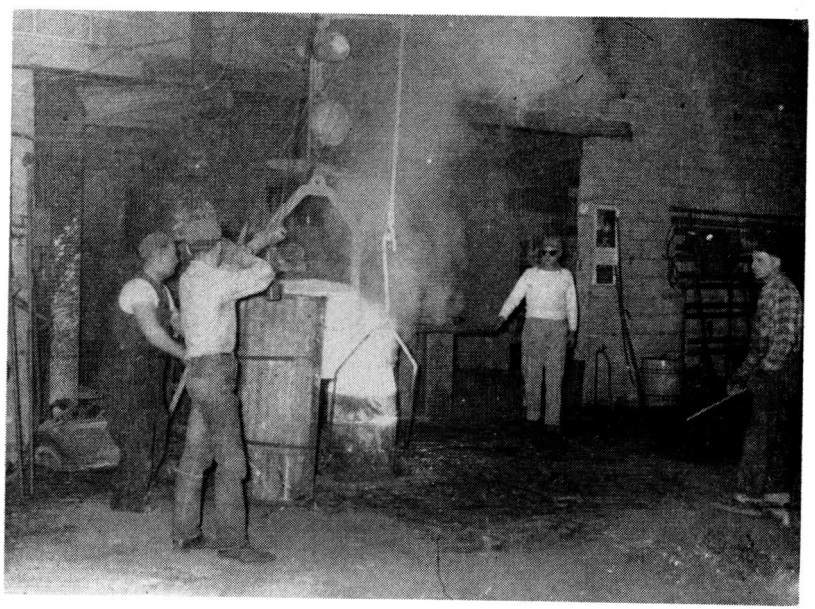

Figure 2. Bottom introduction of magnesium alloy into ductile iron.

3. **Silicon inoculation.** Magnesium addition provides a strong chilling action on molten iron, producing free carbides in the structure of light sections unless care and precision are exercised in the

subsequent inoculation. (By using the Electro-Met alloy, reladling inoculation is not required because of its silicon content.) Ferrosilicon containing at least 72% silicon, with a particle size of about $\frac{3}{8}$-inch diameter, is added to the molten stream of iron during reladling to provide uniform inoculation. The ferrosilicon being dissolved increases the silicon content to such an extent a supersaturated condition with respect to carbon is provided.

4. **Formation of graphite nodules.** A strong graphitizing condition exists that causes precipitation of small nucleating particles of graphite. Work by Gries and Maushake (11) substantiates the theory spheroidal nucleation of carbon is initiated about submicroscopic particles of magnesium oxide, and that carbon nodules grow mainly above the main stems of and within the interstices of primary iron dendrites during solidification.

Spheroidal graphite in ductile iron has a radial polycrystalline appearance and can be readily distinguished from the flake-graphite aggregate intermixed with iron particles that exist as nodules in American blackheart malleable cast iron. The latter are more irregular in shape and a crystalline structure cannot be distinguished under the microscope. Debye-Scherrer patterns indicate an hexagonal crystal structure for the carbon spheroids in magnesium-treated cast iron.

5. **Elements that retard nodulation.** Certain elements have a detrimental effect on the magnesium addition and tend to prevent formation of nodular graphite. Lead is particularly damaging in this respect; 0.002% is the maximum amount that can be permitted in ductile iron. Possible sources of lead would be babbit bearings in scrap engine blocks, or fluorspar, which is frequently used as a flux in the basic cupola or electric furnace. Other elements producing a similar effect include aluminum, antimony, arsenic, bismuth, selenium, tellurium, tin, titanium, and copper. Aluminum and titanium have a stronger effect in producing flake graphite in thick sections than in thin sections. Of course, the toleration amount safely varies in each of the above elements.

6. **Basic cupola production.** The basic cupola is ideal for production of low-sulfur, low-silicon, and high-carbon iron. Iron is not oxidized by this process. The low sulfur content requires using less magnesium alloy for treatment. The Electro-Met alloy is ideal for use in basic practice and provides good as-cast properties. The metal is normally about 100 degrees hotter when tapped from the basic cupola than from the acid cupola. It is very important that a good grade of limestone be used to flux out dirt, sand, and other impurities, and to reduce the sulfur and phosphorus content.

7. **Acid cupola production.** The Eagle Foundry Company uses an acid-lined cupola and, therefore, is quite careful in selecting materials to compose the charge. A charge consists of 34% steel scrap, the remainder being Chilean pig iron and foundry returns. Chilean pig iron contains 0.03 to 0.04% phosphorus, 0.023% sulfur, 0.37% manganese, 1.30% silicon, and 0.23% chromium. Sulfur and phosphorus cannot be removed in the acid process. They *must* be kept low in the charge.

8. **Other means of production.** The Oregon State College foundry poured its initial heat of ductile iron on May 16, 1954. This was produced in the Green electric furnace which was recently installed. This furnace, manufactured by the Green Electric Furnace Company of Seattle, Washington, is a 3-phase, 300 kva, direct-arc furnace with a rated capacity of 400 pounds per hour. The charge for this heat was 100% steel-plate scrap consisting of 400 pounds of steel, 17½ pounds of No. 4 mesh Mexican graphite, 8 pounds of silicon briquettes, 2½ pounds of zirconium-iron-silicon, and 8 pounds of limestone. Liquid iron was tapped at 2925° F. and the reladling treatment was made with 12 pounds of Electro-Met alloy. Iron was poured into the molds at 2400° F., producing gear blanks, caps for a hydraulic cylinder, and ½-inch Y-blocks. Two of the 7¼-inch diameter caps, showing foundry defects repaired by carbon-arc welding, are illustrated in Figure 3.

Other types of furnaces used to produce ductile iron include indirect-arc furnaces, induction furnaces, crucibles, air furnaces, and oil- and coal-fired rotary furnaces. The type of melting unit appears to have little effect on the quality of ductile iron produced. Batch-

Figure 3. Ductile-iron caps for hydraulic cylinder. Repair of foundry defects by carbon-arc welding is shown.

type furnaces, such as the one used at Oregon State College, have a tendency to carburize poorly. Fracture of a chill block during the heat indicated there was insufficient carbon provided by the 16 pounds of graphite in the initial charge. An additional 1½ pounds were added. A subsequent chill test, with a chill about ⅜-inch deep, was considered adequate. The initial carbon and silicon were placed in the bottom of the furnace, underneath the steel, to assure complete solution in the iron. Any undissolved graphite in magnesium-treated iron will develop a mixed graphite structure consisting of flakes and spheroids.

IV. Properties and Uses of Ductile Iron

1. **Quality requirement of welds.** In order to determine the weldability of any metal or alloy, it is essential to have a thorough knowledge of properties in the material itself. While it is always desired to produce a weld with properties that match the parent metal as closely as possible, end use of the article also must be considered.

Cost may be of little consequence for a product that requires the highest physical properties. Requirements of another product might be such that lower mechanical properties are adequate and a less expensive welding process will suffice.

2. **ASTM specifications.** Although several specifications have been used for the purchase of ductile-iron castings, only two are included in the ASTM specifications for nodular-iron castings. These are contained in ASTM designation A339-51T (*2*), and are given in Table 5. The intent of these specifications is to subordinate chemical composition to physical properties. However, composition can be specified also, if desired. In addition to tensile properties, the ASTM specifications include both keel-block and Y-block test coupons, types of tensile specimens, number of tests, heat treatment, workmanship, finish, inspection, and certification.

Table 5. TENSILE REQUIREMENTS FOR DUCTILE IRON

	Grade (80-60-03)	Grade (60-45-10)
Tensile strength, min, psi	80,000	60,000
Yield strength, min, psi	80,000	45,000
Elongation in 2 in., min, per cent	3	10

3. **Strength in compression.** The compressive strength of ductile iron appears to vary directly with hardness. Yield strength in compression ranges from 57,000 psi at a hardness of 219 Brinell to

95,000 psi at a hardness of 321 Brinell (8). International Nickel Company felt information provided by these tests is low since specimens bowed after reaching the yield point and eventually failed in shear.

4. **Impact and fatigue.** Cooper-Bessemer Company investigated impact properties of ductile iron, employing the 0.798-inch diameter Izod test bar used extensively in England (6). Annealed ductile iron absorbed over 120 foot-pounds compared with 50 to 90 foot-pounds for the as-cast condition. These values are comparatively quite high because highly alloyed acicular iron absorbed 20 to 30 foot-pounds, and class 30 gray iron absorbed only from 10 to 14 foot-pounds of energy.

Fatigue resistance of ductile iron is similar to that of ordinary grades of steel in both the notched and unnotched conditions (8). This characteristic, combined with a relatively high constant modulus of elasticity of 25 million psi, and excellent wear resistance, makes it a first-rate material for crankshafts, camshafts, connecting rods, and other parts subjected to stress reversal and wear. The favorable modulus of elasticity and relatively low cost make ductile iron a choice material for rolls for the paper, wrought metal, and rubber industries.

5. **Wear and heat resistance.** One of the outstanding properties of ductile iron is its resistance to wear. A ductile-iron rack and a forged manganese-steel rack were examined after 1500 hours' service at 50% overload (8). The steel rack was pitted and badly worn while the ductile-iron rack was only burnished and in excellent condition. In a gear application involving shock loading, the teeth of gray iron gears broke after two weeks' service. After 4 months, steel gears were worn out. Ductile-iron gears were still providing good service after 8 months' usage. Ductile-iron bearings provided five times the service life of expensive bronze bearings for the rollout table of a steel mill (8).

A surface hardness approaching 600 Brinell can be obtained by either flame or induction hardening of ductile iron. In this condition, for certain die applications its resistance to wear and seizing is superior to any other material used (9).

One objection to many abrasion-resistant materials is their shock sensitivity. A carbidic surface-chilled ductile iron with a shock-resistant core is now used extensively for earth-digging equipment, ore chute liners, and sand and gravel equipment. Scarifier teeth for earth-rooting operations are being produced currently by a local firm. Ductile iron is now used for many parts requiring a high degree

of heat resistance, such as furnace parts and pot liners. Recently a Portland firm rolled into cylinders a number of flat, ⅜-inch thick, ductile cast-iron plates, 6 feet by 3 feet to be used as furnace liners.

6. **Typical uses.** An interesting application of ductile iron where severe shock conditions are encountered is shown in Figure 4. The tractor operator has lifted the front end of the tractor free of the ground by means of the grader blade. Terrific strain is being imposed upon the power arms in service. Ductile-iron power arms, connecting the hydraulic pistons with the grader blade, are now replacing more expensive steel castings.

Ductile cast-iron fittings for irrigation equipment were produced and used, at a reduced cost, to replace aluminum castings. Ductile iron was selected because of its property to resist corrosion and its ability to withstand impact.

A grader blade connection bracket is now used by the Holt Equipment Company to replace a bracket fabricated of welded steel (Figure 5). The company records indicate a substantial savings in cost effected by the use of the ductile-iron bracket. Field service tests show it is performing in a commendable manner.

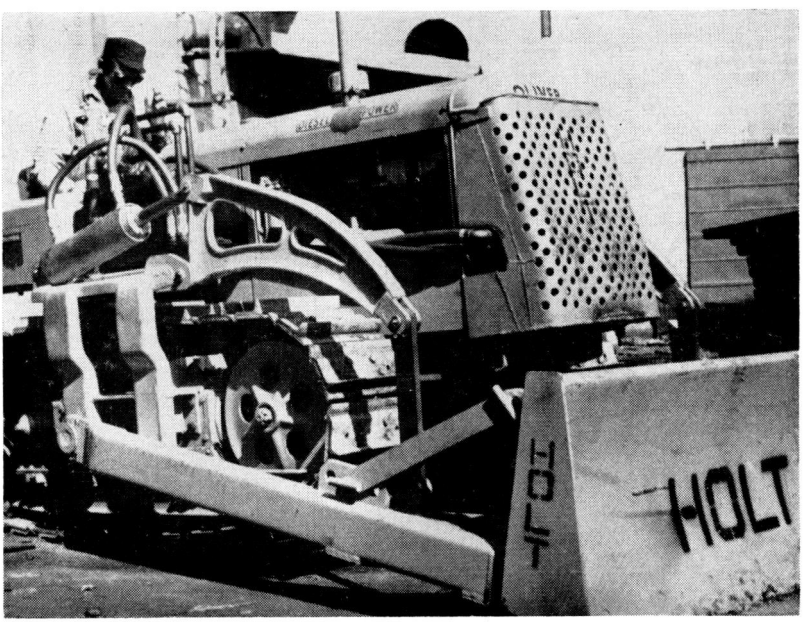

Figure 4. Ductile cast-iron power arm in operation.

Figure 5. Ductile-iron grader blade connection brackets, left and center.

7. **Size of castings.** Apparently there is no limit in the size of ductile-iron castings that can be produced. The Acme Shear Company of Bridgeport, Connecticut is producing ductile-iron electrical hardware fittings weighing less than one-third of an ounce each, in production runs of hundreds of thousands of castings. In contrast with these castings, Chambersburg Engineering Company is producing forging hammer anvils of cast ductile iron weighing 60,000 pounds each.

V. Material Used in the Study

1. **Initial castings.** The preceding general discussion was intended to provide background information that would be of material assistance in conducting the investigation. The following sections pertain directly to the study itself and will enable those who are interested in a continuation of this work to proceed in an efficient manner and without duplication of effort.

The initial castings used for tensile tests consisted of ductile-iron bars 14 inches long, 2 inches wide, and $\frac{3}{8}$-inch thick. These bars had a reduced section $1\frac{1}{2}$ inches wide and 3 inches long at the center to provide a minimum of machining operations on the welds. The shapes of these bars were such that adequate feeding did not take place during solidification and, as a result, extensive microscopic porosity occurred. This porosity, known as centerline or interdendritic shrinkage, also would be prevalent if lower pouring temperatures were used.

2. **Cast rectangular plates.** Although the tensile bars just described were used in a preliminary study of ductile iron welded to steel with nickel-iron electrodes, the test results were of such variable nature that it was deemed necessary to utilize material of greater uniformity in order to obtain higher physical values and more consistent results. It was felt these qualities might be found in flat rectangular plates of larger area and without restricted sections.

Plates with dimensions of 8 inches by 14 inches were then cast in thicknesses of $\frac{1}{2}$-inch, $\frac{3}{4}$-inch, and 1-inch. These plates were radiographed to determine the condition of soundness. All were found to contain extensive areas of interdendritic shrinkage. In addition, the thinner plates contained numerous areas of closely spaced gas pockets, close to the surface of the casting, known as pinholes.

3. **Pinholes.** A section of one of the $\frac{1}{2}$-inch plates in an area of excessive pinholing was removed for microscopic and macroscopic examination (Figure 6). All pinholes appeared to have small openings to the surface. In many instances they could be detected by careful visual inspection of the surface. As a rule, pinholes were detected at the most remote distances from the ingates of commercial castings. However, in the case of flat plates they were adjacent to the ingates. Molding sand, with less moisture content and greater permeability, tends to produce a minimum of pinholes.

When pinholes of as-cast ductile iron were examined carefully, they appeared to have a high carbon coating. Oxidation of this carbon during the annealing process produced an enlargement of the

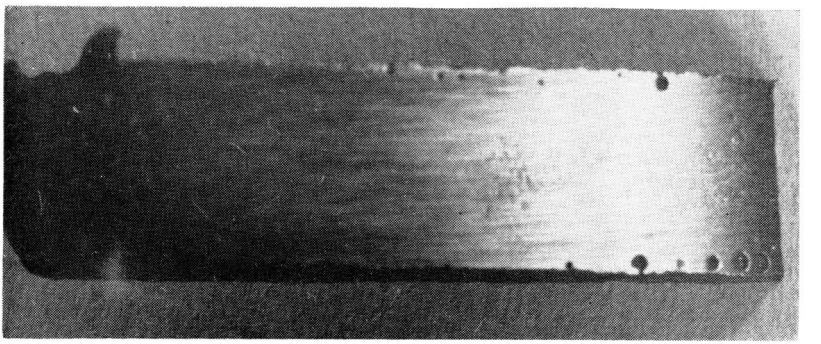

Figure 6. Pinholes and centerline shrinkage.

holes. Increased amounts of graphitizing agents reduced the quantity of pinholes and also produced a minimum of carbidic structure in the as-cast condition.

Although there is little or no published information concerning the cause of pinholes, it appears likely complex iron-magnesium carbides in the molten iron might react with moisture in the sand to produce acetylene gas, which is entrapped in the iron as it approaches solidification. The reasons for this belief are as follows:

1) The odor of acetylene gas can be detected readily in all freshly machined or fractured ductile-iron castings.

2) Pinholing is less prevalent in sands of low moisture content.

3) Pinholing is less prevalent in molds of more permeable sand allowing the escape of gases.

4) Pinholes are connected with the surface of the castings.

5) An increased amount of free carbides in the as-cast structure appears to be associated with pinholing.

Holt Equipment Company received information from the International Nickel Company to the effect additions of either tellurium or aluminum would counteract pinholing. Holt Equipment Company has virtually eliminated pinholes by the addition of tellurium, which was purchased in pellet form from the American Smelting and Refining Company. The required amount of tellurium was about one gram per 100 pounds of ductile iron. Increased quantities of tellurium promoted surface roughness and also retarded the formation of spheroidal carbon.

There is some industrial hazard involved in the use of tellurium since its fumes are harmful to workmen. It should be used only when adequate ventilation is provided.

4. **Cast Y-blocks.** After examining the cast plates it appeared very doubtful if their quality was sufficient to produce valid test results. This possibility had been foreseen, however, in working with the previous test bars and, as a consequence, patterns also had been made for test Y-blocks that would provide both 1-inch- and ½-inch-thick test sections. These blocks, shown in Figure 7, provided test sections 14 inches long and 2½ inches wide, with a continuous feeding reservoir or riser above the casting that could be removed by cutting with a power bandsaw.

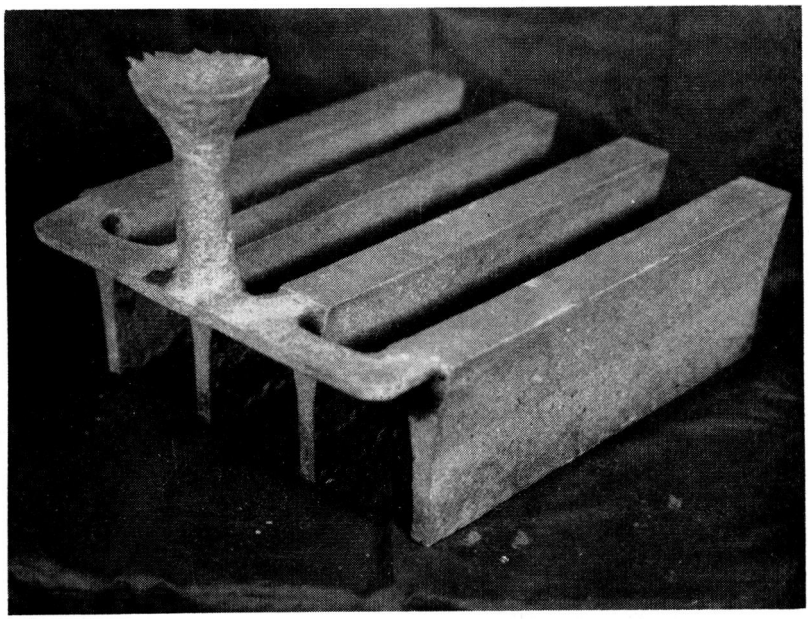

Figure 7. Gating system for ductile-iron Y-blocks.

5. **Properties of Y-blocks versus rectangular plates.** Both tensile and flexure tests were made of the plate material and the Y-block test sections in order to determine "effect of shape of casting" on the physical properties. Specimens B-11 and B-12, (Figure 8), were from the ½-inch plate, and B-3 was from a ½-inch Y-block. All were poured from the same heat and were in the annealed condition. Specimen B-11 failed at 42,000 psi ultimate strength with an elongation of 1.5%, while B-12 failed in the grips rather than in the reduced section. Specimen B-3 failed at 68,000 psi ultimate strength with 17% elongation. Figure 9, which shows the

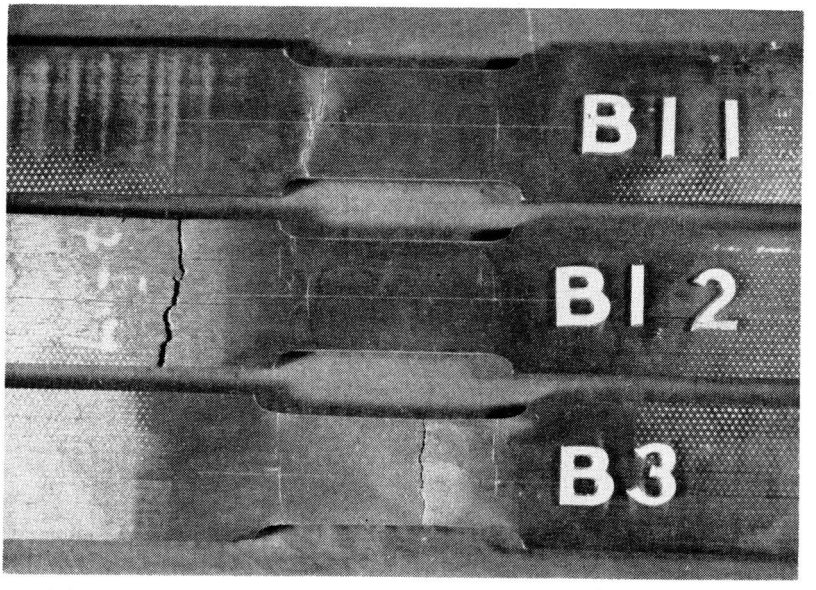

Figure 8. B-11 and B-12 of ½-inch plate and B-3 of Y-block.

fractured ends of these bars, indicates a more homogenous structure for specimen B-3.

Flexure tests were made on rectangular bars 1½-inches wide and ¾-inch thick, in the annealed condition. Third-point loading was applied between knife edges spaced 12 inches apart. Specimen B-52 was from an area with excessive centerline shrinkage of the 1-inch thick plate (according to the radiograph), while specimen B-51 was selected from the section of plate with maximum soundness. Results of these tests are shown in Figure 10, together with specimen B-6 from a 1-inch Y-block from the same heat.

The fractured ends of the flexure test bars (Figure 11), show the dark areas of centerline shrinkage in specimens B-51 and B-52 to be predominantly in the cope side of the plate, which is the last portion to solidify. Dark areas in these specimens should not be confused with the dark area in specimen B-6, which is finer grained, lighter in color, and does not represent centerline shrinkage. Metallographic specimens of B-6, shown in Figure 12, disclose no difference in microstructure between dark and light areas. The difference is due to light reflection. The side in tension provided a rough surface with more light absorption, while the compression side provided a less ductile type of fracture that crossed several grains

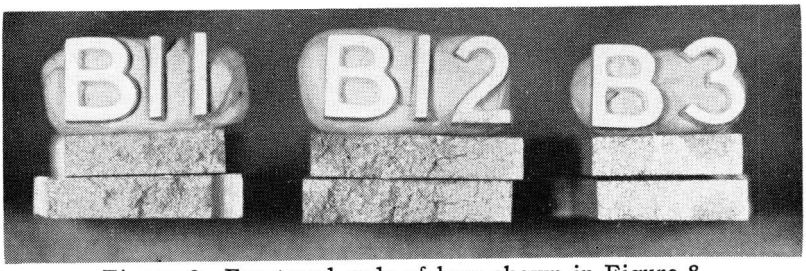

Figure 9. Fractured ends of bars shown in Figure 8.

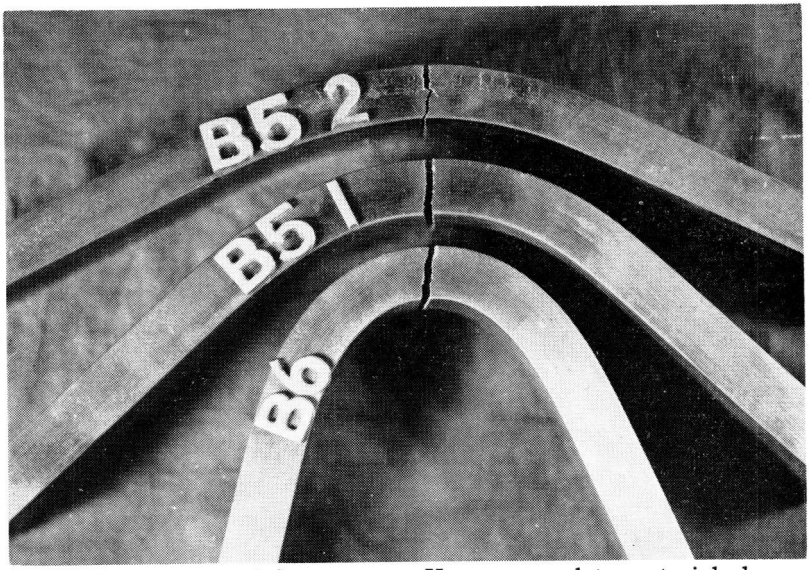

Figure 10. Results of flexure test. Upper, two-plate material; lower, Y-block.

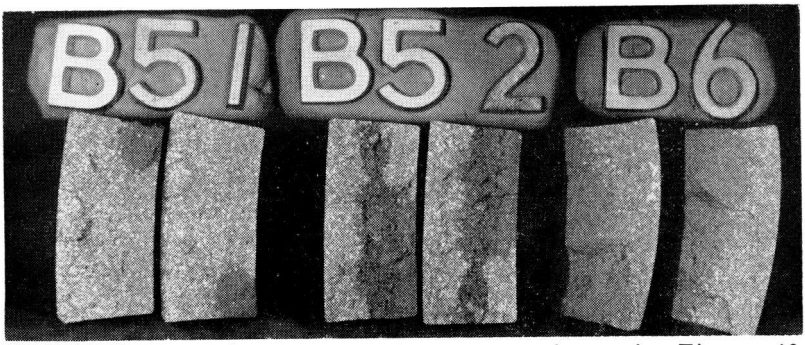

Figure 11. Fractured ends of specimens shown in Figure 10.

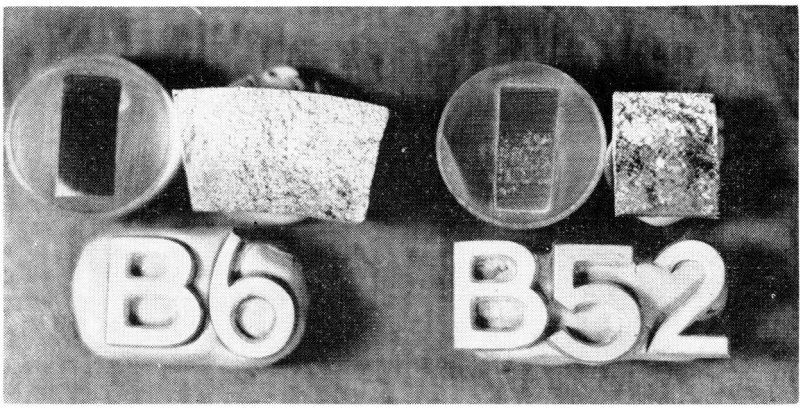

Figure 12. Metallographic specimens with centerline shrinkage shown in B-52.

at a time without change of direction, thereby providing good light reflection. The etched section from specimen B-52 clearly shows that centerline shrinkage in this case is of macroscopic magnitude.

Evidence provided by the tests just described indicates Y-blocks were necessary in order to produce the required quality of material for this investigation. This was a disadvantage in that the plate material could be processed far more rapidly and would permit a broader scope of the testing program.

6. **Drossy fractures.** Several castings produced drossy or sooty areas in the fractures as a result of graphite stringers associated with oxysulfide and silicide slag, caused by oxidation of iron and magnesium sulfide. Due to this condition, which was ascertained by X-ray examination, it was necessary to reject a large percentage of the earlier test castings. White, defective areas are shown in the print of a radiograph of a rejected Y-block casting. (See Figure 13.)

Figure 13. Print of radiograph of defective Y-block.

This condition was somewhat mitigated by use of higher pouring temperatures. From this standpoint, iron from the fourth tap of the day's heat, and from the first to be poured from the ladle, was considered to be best. More careful skimming of slag and the use of ladles constructed to provide bottom pour of iron also helped to improve the quality of castings.

7. **Gating system.** Four castings were produced per mold. The gating system of these is shown in Figure 7. A system involving the use of a pouring basin with a skim gate would be far superior to pouring directly into the sprue, as shown. The use of bottom gating with slag traps would also produce castings of greater soundness. These practices did not appear to be feasible under the production setup used in making the castings shown. However, due to a continued high rate of rejected castings, slag traps were used eventually in the inlet between gate and casting, which greatly improved the general quality of the castings.

8. **Cast T-beams.** T-beams having a 2-inch flange and a 2-inch web, each $\frac{3}{8}$-inch thick, were cast in 16-inch lengths for use in the flexure tests. All of these bars had extensive centerline shrinkage at the intersection of web and flange, with random areas of shrinkage in the flange that interfered with good correlation of test results. This is illustrated in Figure 14 by the dark areas in a broken T-beam. As a consequence, these bars were used only to a minor extent in the program.

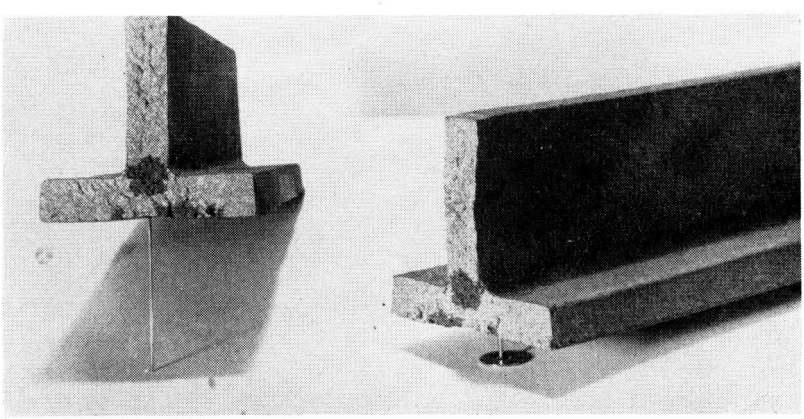

Figure 14. Fractured T-beam showing dark areas of centerline shrinkage.

VI. Preparation of Test Specimens

1. **Preheating of castings.** Because of the high carbon content in ductile iron, it is desirable, in order to avoid fusion-zone cracking, to use a minimum preheat of 500° F. when it is to be welded. While this is not mandatory for simple shapes with single-pass welds, complicated castings and multiple-pass welds frequently require preheats well in excess of 500° F. This is particularly true when iron-base electrodes, or electrodes of large diameters are used, requiring higher current settings.

A simple and expedient method of preheating castings was afforded by means of a preheating table with a firebrick top 32 inches square. This table, shown in Fgure 15, was fabricated of welded steel pipe and angle iron and located immediately adjacent to the welding booth in order that the effect of preheat would not be lost during the transfer of specimens. When mounted on heavy industrial casters for portability, the table had a convenient working height of 32 inches.

The preheat burner is shown in operation in Figure 15. Air and gas could be regulated to provide flame of any type or intensity that was desired. To provide a furnace to suit each individual job,

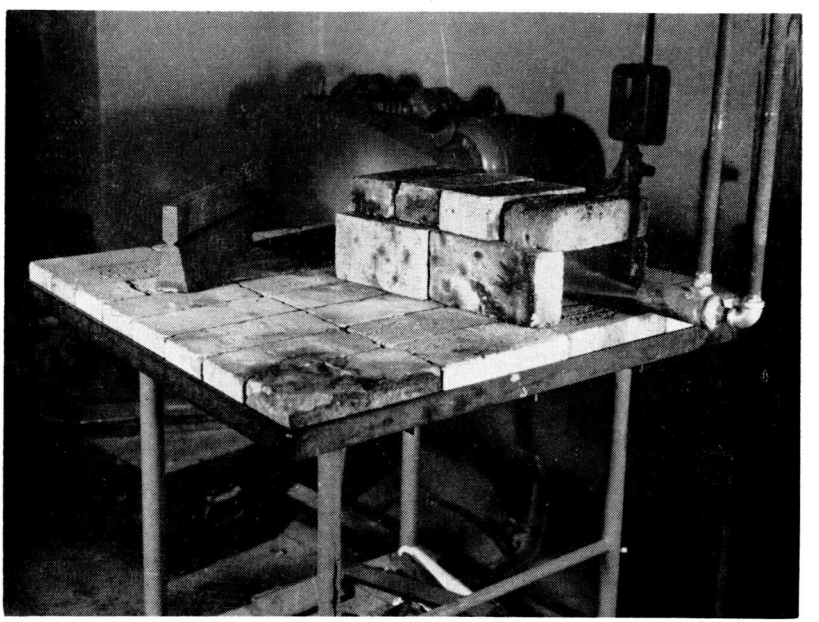

Figure 15. Table and burner for preheating castings.

loose firebrick could be arranged around any size or shape of casting that the table top would accommodate.

2. **Alignment for welding.** An alignment and positioning fixture for the specimens to be welded (Figure 16), was fabricated of 6-inch channel iron. This fixture, 14 inches long and 8 inches wide, provided a fast and positive alignment of pieces to be welded and a support with ready accessibility during welding operations. Rigidity of the fixture was such that no warpage was experienced during any of the extensive welding operations. The test section on the fixture had just been welded and was of as-cast ductile iron welded with the carbon arc, using ductile-iron filler rod.

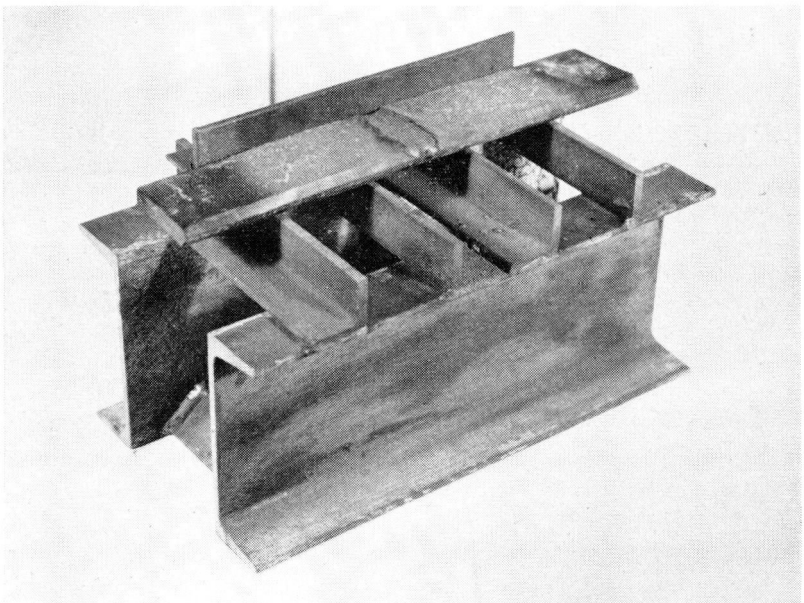

Figure 16. Positioning fixture for welding Y-blocks.

3. **Radiography of castings.** All castings used in the testing program were first radiographed. Only those completely sound and free of defects were utilized. A mechanically rectified, 200 kilovolt, Victor X-ray machine, equipped with a General Electric oil-cooled tube, was used for the radiographic work. This equipment was operated at the maximum setting to permit continuous operation at 174 kilovolts and a tube current of 26 milliamperes. The gamma ray, consisting of a 50-milligram capsule of radium, was used initially

for castings 1 inch in thickness. X-ray equipment provided more satisfactory results, however, and use of the gamma ray was discontinued.

Both Eastman type K and type A film were used for radiographing the $\frac{1}{2}$-inch thick sections. Type K film had the greatest speed of any X-ray film used. Four-minute exposures were required for $\frac{1}{2}$-inch thick ductile iron when leadfoil screens were used. Leadfoil screens diminished the effect of scattered radiation, producing greater contrast and clarity of image. Exposure time for material of that thickness and density was also reduced slightly. The relative speed of type K film was four times greater than that of type A. To reduce exposure time it became necessary to use calcium-tungstate intensifying screens when using type A film. Using $1\frac{1}{4}$-minute exposures with type A film and the calcium-tungstate screens was equivalent to 4-minute exposures with type K film and leadfoil screens. X-rays caused calcium tungstate to fluoresce and the light emitted intensified exposure of the film. Approximately one-thirteenth of the normal exposure time was required when intensifying screens with type A film were used. Intensifying screens produced graininess in the developed film which interfered somewhat with detection of minute defects. Improved contrast of the slower type A film over type K more than compensated for this. Consequently, superior negatives were produced.

Fifteen-minute exposures for 1-inch-thick ductile iron were required when using type K film with calcium-tungstate intensifying screens. Slower type F film, which was particularly adapted to intensifying screens, required only 12-second exposures for the same castings.

Careful blocking was required over all portions of the cassette not covered by the casting to be radiographed because a very small area of free radiation on one portion of the intensifying screen fogged the entire film. Although blocking was desired in all cases, it was not found essential when leadfoil screens were used. Although special X-ray film developer was recommended, D-19 developer provided satisfactory results if the time of development was increased by about one-half of that recommended for ordinary film.

4. **Ductile iron welded to steel.** A frequent industrial fabrication requirement of ductile-iron castings is that they be integrated with wrought steel shapes in the production of machinery parts. A minor portion of this study, therefore, concerns the properties of welds connecting ductile iron with steel.

The $\frac{3}{8}$-inch thick reduced-section tensile bars, described in the previous chapter, were sectioned at the center and each piece was

welded to a ⅜-inch thick by 2-inch wide steel bar to provide rectangular reduced-section tensile test bars 14 inches long. In preparation for welding, ends of both pieces were ground to form a double-V butt joint with a 60-degree included angle. All surface skin and scale were removed by grinding adjacent to the weld to prevent contamination of the weld. These welds were made with Ni-Rod 55 electrodes, using direct current with the electrode positive. A minimum preheat of 500° F. was maintained during the welding process. Slag was thoroughly removed from each pass prior to deposit of the weld metal.

Flexure test specimens also were prepared of ductile iron welded to steel, using T-beam sections described in the previous chapter. Steel T-beams, 8 inches in length, were fabricated by welding together 2-inch by ⅜-inch mild-steel bar stock with fillet welds, using 3/16-inch diameter E6012 electrodes with direct current, straight polarity, and a current setting of 165 amperes. The ductile-iron T-beams were fractured in flexure to determine property of the parent metal. Ends of the broken bars and ends of the fabricated steel bars were then bevel ground to form double-V butt joints, with a 60-degree included angle for welding. All scale was removed adjacent to the weld that was to be made. Bars were preheated to 600° F. prior to welding. All the T-beam sections shown in Figure 17 were welded with Ni-Rod 55 electrodes in the same manner as the tensile test bars.

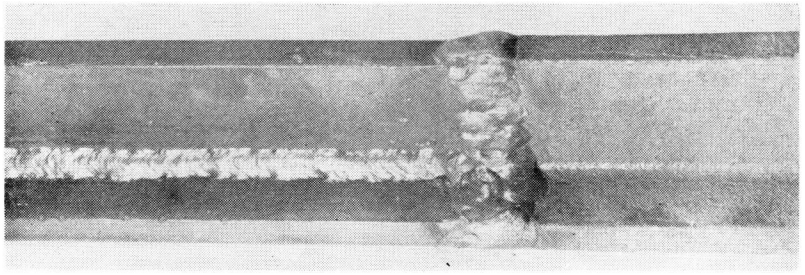

Figure 17. Two-inch, T-beam flexure test specimen consisting of ductile cast iron welded to steel.

For subsequent studies in weldability of ductile iron, it was decided to discontinue use of the shapes just described and to use Y-block material because of its more consistent quality.

International Nickel Company, which had conducted some exploratory work in this field, was consulted in regard to the most desirable program. Their recommendations, together with other reasonable possibilities, were followed.

5. **Heat treatment.** In the Pacific Northwest, virtually all ductile iron is used in the annealed condition at the present time. For this reason it was decided that testing of welded as-cast material would be of minor economic importance. Emphasis was placed, therefore, on testing castings that had been annealed prior to welding; also on castings that had been reannealed after the welding operation, to determine if this would provide material advantages. Welding of material in the as-cast condition, followed by annealing, was also included in the program as this would provide economic advantages in the foundry repair of defective castings.

Table 6. SCHEDULE OF WELDING AND HEAT TREATMENT OF DUCTILE IRON

Specimen design	Welding process and electrode	Heat treatment
A-1		As cast
B-1		Normalized
B-2		Normalized
C-1	Arc, 18-8 Cr-Ni stainless steel	Annealed, not preheated
C-2	Arc, 18-8 Cr-Ni stainless steel	As cast; preheated, welded, then annealed
D-1	Arc, E6015, low-hydrogen mild steel	Annealed, not preheated
D-2	Arc, E6015, low-hydrogen mild steel	Annealed, preheated
D-3	Arc, E6015, low-hydrogen mild steel	As cast; preheated, welded, then annealed
D-4	Arc, E8015, low-hydrogen	Annealed, welded, then reannealed
E-1	Arc, 25-20 Cr-Ni stainless steel	Annealed, not preheated
E-2	Arc, 25-20 Cr-Ni stainless steel	Annealed, preheated
E-3	Arc, 25-20 Cr-Ni stainless steel	As cast; preheated, welded, then annealed
F-1	Oxyacetylene welded, parent metal filler rod	Annealed, preheated
F-2	Oxyacetylene welded, parent metal filler rod	As cast; preheated, then annealed
G-1	Heliarc welded, parent metal filler rod	Annealed, preheated, welded, then reannealed.
G-2	Heliarc welded, parent metal filler rod	As cast; preheated, welded, then annealed
H-1	Arc, Ni-rod 55	Annealed, not preheated
H-2	Arc, Ni-rod 55	Annealed, preheated
H-3	Arc, Ni-rod 55	As cast; preheated, welded, then annealed
I-1	Arc, E6013, mild steel	Annealed, not preheated
I-2	Arc, E6013, mild steel	Annealed, preheated
I-3	Arc, E6013, mild steel	As cast; preheated, welded, then annealed
J-1	Oxyacetylene brazed, manganese-bronze filler rod	Annealed, brazed, no preheat
K-1	Carbon arc, parent metal filler rod	Annealed, preheated, welded, then reannealed

6. **Scope of investigation.** Scope of the investigation included metallic-arc welding with both ferrous and nonferrous electrodes, inert gas-shielded arc welding, and carbon-arc welding. It also included oxyacetylene fusion welding and brazing. The complete schedule of welding and heat-treating operations, together with the specimen designations, is given in Table 6.

The original schedule of operations for preparation of castings for welding was as follows:

1. Anneal castings 5 hours at 1650° F. followed by furnace cooling through 1250° F. at a rate not to exceed 35 degrees per hour.
2. Clean castings by tumbling to remove scale, sand, or other foreign material adhering to the surface.
3. Radiograph to determine quality of casting.
4. Cut test section from feeder Y-section by means of a power bandsaw.
5. Bevel casting as required for welding.

7. **Machining of parent metal test specimens.** Parent metal tensile test specimens were prepared from numerous heats in order to obtain correlation with welded specimens of similar composition. Test bars were machined from the $\frac{1}{2}$-inch thick Y-blocks to cross sections of $1\frac{1}{2}$ inches in width and $\frac{3}{8}$-inch or greater in thickness, with machining marks parallel to the length. Because the gage length was limited to 2 inches, a reduced section $1\frac{1}{4}$ inches in width was then milled with a $2\frac{1}{2}$-inch diameter milling cutter to avoid stress concentrations. These specimens were prepared in both the as-cast and annealed conditions.

Rectangular tensile test bars having approximately the same area and standard 0.505-inch diameter test bars with 2-inch gage lengths also were prepared from representative samples of 1-inch thick Y-blocks in both the as-cast and annealed conditions. Standard, unnotched, impact specimens 0.394-inch square also were prepared from the above material.

8. **Joint preparation for welding.** All specimens to be fusion welded were beveled at the center to form double-V butt joints, with included angles of 60 degrees. Although a greater included angle, usually 90 degrees, has been used frequently for oxyacetylene welding, the thickness was not sufficient in this case to make an appreciable difference. An exception in joint preparation was made in the case of bars to be brazed. In these, a shear V-joint was prepared to provide additional surface.

In brazing it is necessary to establish a surface bond between the parent metal and the deposited metal, and strength can be obtained

only by means of special joint preparation. To prevent contamination of the weld deposit, all surface scale was removed by grinding for a distance of about ½ inch from the prepared joint.

9. **Welding with AWS 308-15 electrodes.** The first ferrous welding electrodes used were type AWS 308-15 stainless steel containing 18% chromium and 8% nickel. Bars to be welded were preheated to 800° F. and the heat of welding was sufficient thereafter to maintain this temperature in the joint area of the base metal.

Beads were successively deposited on alternate sides of the joint, with sufficient weaving to permit flow of weld metal to each side of the joint in each pass. Electrodes ⅛-inch in diameter were used for the root beads, with a current setting of 90 amperes. Electrodes 5/32-inch in diameter were used for the remaining passes, with a current setting of 130 amperes. Complete slag removal was effected on each pass prior to deposit of the weld metal. The flow of weld metal was smooth, providing even deposit of metal and ease of manipulation of the electrode. Following the welding operation, specimens were prepared of annealed ductile iron both as welded and reannealed.

Flexure test specimens were prepared for welding from 1-inch Y-block material in the same manner as that described for tensile tests of ½-inch thick material. These bars also were welded with type AWS 308-15 stainless electrodes, using the same procedure as for the tensile test bars.

Results of these tests, which will be discussed later, were of such nature that it was decided to discontinue further flexure tests until the entire tensile testing program was completed.

10. **Low-hydrogen steel electrodes.** Low-hydrogen mild-steel electrodes of the E6015 type were then used in the preparation of test specimens. Some of these specimens were welded without benefit of preheat, while others were preheated as previously described.

Electrodes of ⅛-inch diameter were used for root beads; 5/32-inch diameter electrodes for the remaining passes. Each size of electrode required about 10 amperes more current than necessary for the type 308 stainless electrodes of corresponding size. This created a problem of greater admixture of weld and base metal. Care was taken to permit the weld metal to roll against the sides of the "V" during the weaving manipulation rather than to permit direct contact between the arc and the parent metal. The current setting for this type of electrode was quite critical because, although a minimum current was definitely preferred, there was a greater tendency for slag entrapment at lower amperage values. Welds with this type

of electrode were made in the as-cast condition followed by annealing, in the annealed condition as welded, and in the annealed condition followed by a reanneal. Welds also were made on material containing less than 3% and more than 4% silicon in order to determine effects of this element on fusion zone cracking.

11. **AWS 310-15 electrodes.** Stainless-steel electrodes of the AWS type 310-15, containing 25% chromium and 20% nickel, were used in the preparation of test specimens to determine the advantage, if any, of an increased alloy content of weld metal. The welding procedure and current settings were similar to those for type 308-15 electrodes. These electrodes provided the greatest ease of manipulation and smoothness of transfer of weld metal of any type used, either earlier or later in the program. Specimens were prepared for test purposes both in the annealed as-welded and in the annealed, welded, and then reannealed conditions.

12. **AWS E6013 electrodes.** The final types of ferrous electrodes used in welding ductile iron for test purposes were the AWS E6013. These were straight polarity, mild-steel electrodes with shallow penetration into the base metal due to a soft, nondigging type of arc. This characteristic was provided by a high ratio of potassium silicate to sodium silicate in the coating. This type was selected among the mild-steel electrodes with coatings that contain organic materials because it would provide a minimum of carbon pickup from the base metal. In addition, the high titania-potassium silicate content of the coating, with a corresponding reduction of cellulose, provided less hydrogen to react with the base metal than AWS E6010 or E6011 electrodes.

The characteristics of weld-metal transfer for this type of electrode were of such nature that lower current settings could be used than for the previously discussed types. A current setting of 80 amperes was used for $\frac{1}{8}$-inch diameter electrodes, and 110 amperes for 5/32-inch diameter electrodes.

A noticeable boiling reaction took place as the weld metal was deposited. This was attributed to the probable formation of acetylene gas caused by a reaction between moisture which this type of coating contains and carbides in the weld metal, due to the sudden carbon pickup from the base metal. When slag was removed from the weld metal, the deposit was porous and rough. It was readily apparent, even before testing, that weldability of ductile iron with this type of electrode was very poor.

13. **Ni-Rod 55 electrodes.** A number of test bars were welded with Ni-Rod 55, an electrode consisting of core wire containing 60%

nickel, 40% iron, and with an extruded carboniferous limespar coating. This electrode was particularly recommended by the manufacturer for welding of ductile-iron castings. Root passes were deposited with $\frac{1}{8}$-inch diameter electrodes at 85 amperes and intermediate open-line voltage. Remaining passes were made with 5/32-inch diameter electrodes at 105 amperes. All passes, excepting root beads, were made by weaving to the full extent of the width of joint rather than by deposit of stringer beads.

This electrode had excellent operating characteristics and the base metal responded well to its application. The low current setting provided a minimum of alloying between parent metal and the weld. The material was welded in the annealed condition without benefit of preheat; also in the preheated as-cast condition followed by an anneal.

14. **Inert gas-shielded arc process.** For heliarc welding, a 600-ampere alternating current welding machine was used with a superimposed high frequency current for stabilization of the arc and for ease of striking and maintaining an arc without touching an electrode to the parent metal. A $\frac{1}{8}$-inch diameter thoriated tungsten electrode, contained within a size No. 8 ceramic cup, provided the arc for welding heat. Argon, an inert gas, was passed through the cup at a rate of 22 cubic feet per hour to surround the weld deposit and protect it from atmospheric contamination. The electrode holder was protected by water cooling. Gas was regulated by means of a flow meter.

A filler rod from parent metal of a composition similar to that to be heliarc welded was cut into approximately $\frac{1}{4}$-inch square bars by means of a bandsaw. The parent metal was preheated to 1000° F. and welded on the preheating table in order to maintain a high temperature in the base metal during the welding operation. A rather high current of 200 amperes was used to effect a rapid deposit of weld metal. All specimens were reheated to 1000° F. for 5 minutes immediately following the welding to eliminate a condition of stress.

Excellent weldability was experienced by this process and the welds were completed at a more rapid rate than by any other means. Flux was not required because oxides were readily floated to the surface due to the fluid condition provided by the high welding temperature. Specimens were welded both in the as-cast and annealed conditions, and all welded specimens were given a full postweld anneal.

15. **Carbon-arc process.** The microstructure of the heliarc-welded specimens disclosed a partial reversion to a quasi-flake

graphite that reduced the mechanical properties. This was attributed to the high temperature involved in the welding process. It was decided, therefore, to use a minimum of current during the operation of carbon-arc welding. Cored carbon electrodes of $\frac{1}{4}$-inch diameter were used with the electrode negative, direct current, at 120 amperes and high open-line voltage. Flux was not required as the fluidity of the welding puddle was such that oxides were readily floated to the surface. A parent metal filler rod was used and the welding technique was similar to that of oxyacetylene welding, with the exception that speed of the carbon-arc welding was much greater.

If the layer of deposited metal was too thick, even when high preheats were maintained, there was a tendency for hot cracks to form in the center of the weld. This was easily avoided by depositing less metal per pass. A special carbon-electrode holder was not available. It was necessary to periodically immerse the conventional type of electrode holder in water to prevent overheating. The material welded was annealed ductile iron. It was reannealed after welding.

16. **Oxyacetylene process.** A parent metal filler rod also was used with the oxyacetylene welding process as were two popular brands of cast-iron welding flux. Neither was very effective, however, in the removal of oxides formed during the welding process. The best technique, under the circumstances, was to use sufficient heat to enable the rod to be retained in the molten pool and to maintain a puddling action without disturbing the surface film of oxide. The high carbon content of the weld produced a relatively low melting condition, near the eutectic, and the oxides formed had a higher melting point. Failure of the flux to adequately lower the melting point provided a viscous surface condition that prevented complete gas escapement. As a result, gas pockets existed in the surface layers of the weld and, to some extent, deeper within the weld. It is recommended that further experimentation be conducted on the correct flux to use if extensive oxyacteylene welding is to be done on ductile iron. All oxyacetylene welding was done on annealed ductile iron. Some of the specimens were given a reanneal prior to testing.

17. **Brazing.** Ductile-iron test bars prepared with a shear V-joint were bronze welded with an Oxweld No. 25M manganese-bronze filler rod. The oxyacetylene flame was adjusted until slightly oxidizing to eliminate gas pockets in the deposited metal. No preheat was used or considered necessary. This function automatically took place while bringing the pieces up to tinning temperature with the torch. The joint was tinned with a $\frac{1}{8}$-inch diameter rod, using a high-temperature brazing flux. The weld was then completed with a 3/16-

inch diameter flux-coated rod. All specimens were annealed prior to brazing. No subsequent heat treatment was given.

18. **Machining of welded test specimens.** All welded tensile test bars were machined to rectangular cross sections of about $1\frac{5}{8}$-inch width by $\frac{3}{8}$-inch thickness. A reduced test section was then milled or shaped to a $1\frac{3}{8}$-inch width, with a $1\frac{1}{4}$-inch radius to provide a 2-inch gage length on each bar. Those specimens readily machined had the reduced section milled. Those requiring carbide tools for machining were shaped to provide the reduced section. Flexure test bars, with exception of the T-beams, were machined to a rectangular cross section of $1\frac{1}{2}$-inch width and $\frac{3}{4}$-inch thickness. The composite welded T-beams were not machined. Impact specimens were machined according to ASTM specifications, but were not notched.

Both fusion zones and weld zones of specimens welded with mild-steel and stainless-steel electrodes were exceedingly hard. Carbide tools were required to satisfactorily machine these bars and, even then, periodic sharpening of the tools became necessary. Carbide tools were also required for oxyacetylene-welded material that was not subsequentally annealed.

All ductile iron welded by the carbon arc, inert gas-shielded arc, or the oxyacteylene flame, using parent metal filler rod, was readily machined with high-speed cutting tools, provided a post-weld anneal was applied. All brazed material was readily machined with high-speed steel tool bits. Castings welded with Ni-Rod 55 could be machined with difficulty when high-speed tools were employed. Carbide tools were much preferred, however.

After test specimens were machined, test sections were sanded on a belt sander and draw-filed longitudinally to remove any tool marks remaining from the machining process. Corners were slightly rounded and 2-inch gage marks were applied to test sections. Specimens were then ready for mechanical testing.

VII. Metallography of Welded Ductile Iron

1. **Purpose of microscopic examination.** Numerous advantages are offered by a metallographic study of welds. An examination of structure enables one to understand the extent to which integration has taken place between weld and base metal. The effect of welding heat upon the base metal, the alteration products existing in the fusion zone, the nature of defects and inclusions, and many other problems are solved by microscopic examination. It assists in the interpretation of test results. Prior to testing one can predict many physical properties with reasonable accuracy.

2. **Preparation of specimens.** Specimens were prepared for metallographic study from welds made with each process, type of filler rod, and condition of heat treatment.

Procedure for dry polishing consisted of first surfacing the specimen on a belt sander equipped with a 240 grit belt. It was then polished in succession on numbers 1/0, 2/0, and 3/0 emery paper, with an application of graphite applied to the 3/0 paper to help prevent removal of the nodules. Very little trouble was experienced in retaining the carbon nodules prior to the wet-polishing operations.

Wet polishing was accomplished by means of a silk-covered wheel, using levigated alumina as an abrasive. The specimen was etched with 2% nital and repolished several times until all scratches were removed. Nodules were retained in this manner, but they were slightly depressed at the center, with their structures somewhat obscured.

Because results of the wet-polishing operations are not entirely satisfactory, use of a very fast-cutting abrasive is suggested. For this purpose, the Buehler Diamet-Hyprez diamond dust compound offers good possibilities. The procedure would be to follow the 3/0 emery polishing paper with 600X alundum on waxed billiard cloth. The final polishing operation would consist of using 1/4-micron diamond dust on microcloth.

3. **Structure of parent metal.** An examination was made of the parent metal in the as-cast condition at a magnification of X500 (Figure 18). As cooling progressed from the liquid melt, gamma iron saturated with carbon was the first to solidify. As cooling continued, silicon, dissolved in the austenite, caused a reduced solubility for carbon which, nucleated by minute particles of magnesium oxide, formed graphite nodules in the gamma-iron areas. The last portion to solidify formed a network of eutectic consisting of cementite and gamma iron around the primary austenite.

Twin nodules of graphite may be noted in Figure 18. The gamma iron with which they were surrounded formed coarse pearlite upon cooling below the transformation temperature. Examination of a broad area disclosed that, as the material cooled from the solidus and the solubility of carbon in austenite decreased, stringers of iron carbide precipitated out in the austenite areas to form a Widmänstatten pattern. The section of casting examined was relatively thin and the cooling rate sufficiently rapid to prevent excess carbon from migrating to the nodules. This represented a brittle condition which could be eliminated by annealing.

Standard procedure for annealing included heating for 5 hours at 1650° F., followed by very slow cooling through the transforma-

Figure 18. Ductile iron, as cast. X500.

tion temperature. During the 1650° F. treatment, all of the excess carbon (shown as carbides in Figure 18), had time to migrate to the nodules, which were surrounded by gamma iron saturated with carbon. As cooling took place slowly, and the solubility of carbon in gamma iron decreased, the carbon migrated to the nodules. With very slow cooling during transformation, all remaining carbon in the gamma iron moved to the nodules, creating a completely ferritic matrix which was quite soft and ductile, as shown in Figure 19 at X100.

A specimen of ductile iron was removed from the furnace and air cooled after it had been held at 1650° F. for 5 hours. The normalized structure thus obtained is shown in Figure 20 at X500.

Very little time was afforded during cooling for migration of the carbon to the nodules from any distance. Some carbon-free ferrite existed around almost all of the nodules. The matrix consisted of fine pearlite, some of which was well resolved (Figure 20). Carbon appeared to migrate to the nodules quite rapidly along grain boundaries, and to a lesser extent along certain preferred planes within the grain itself.

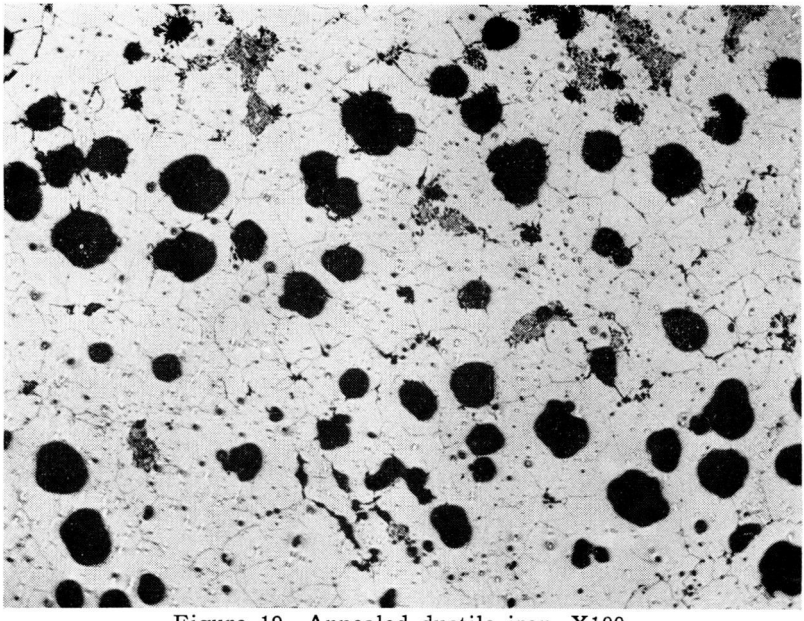

Figure 19. Annealed ductile iron. X100.

Figure 20. Normalized ductile iron. X500.

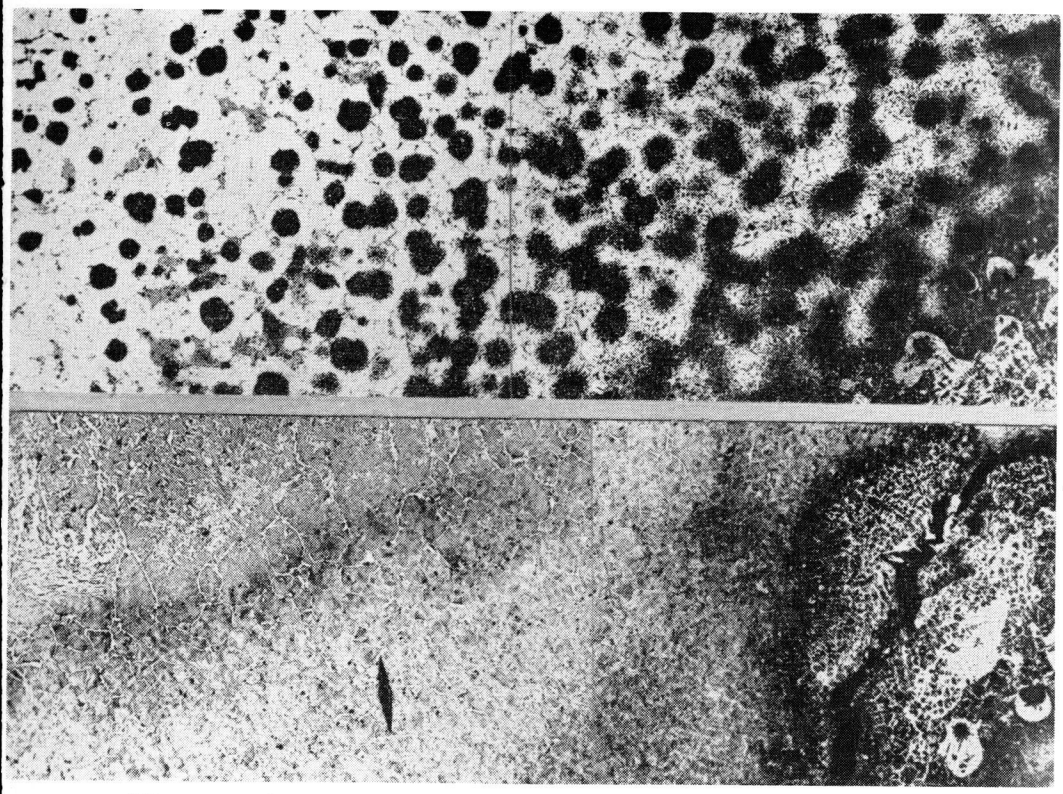

Figure 21. Panorama of ductile iron as welded with E6013 electrodes. X50.

4. **Welded structures using E6013 electrodes.** Results from the use of mild-steel electrodes in welding ductile iron illustrated the nature of some of the more serious problems.

A panorama extending from the as-welded base metal into the weld zone is shown in Figure 21 at X50. At the upper left, parent metal was not heated above the critical temperature by the welding process. At the center of the same figure, the base metal was heated to just above the critical temperature and carbon started to diffuse from the nodule into the surrounding austenite. Transformation products resulted when heat was rapidly conducted away by the base metal.

As the weld was approached (Figure 21), the temperature became increasingly higher and more transformation products sur-

rounded the nodules in areas where carbon had diffused. At the extreme right, where very fine pearlite was present, sufficient carbon diffused to saturate the austenite adjacent to the nodules. In the lower right portion, nodules were surrounded by a white area. The temperature there was just above the solidus, and the carbon-saturated area surrounding the nodule melted because it was of eutectic composition. Upon cooling, iron carbide existed, surrounded by austenite transformation products, including martensite.

The lower portion of the panorama (Figure 21) extended from the fusion zone at the right into the weld zone at the left. At the extreme upper right, liquids surrounding the nodules met and they were completely dissolved. A hypereutectic condition existed in the area of the nodule, which was surrounded by a metal of hypoeutectic composition. Carbon migrated rapidly from this area into the low-carbon, steel-weld deposit at the left, increasing it to an eutectoid composition. At the left, farther into the weld, carbon content was slightly lower and a small amount of ferrite existed around the high-carbon pearlitic areas.

An extensive crack existed in the parent metal just beneath the weld deposit (Figure 21). Coating of the E6013 electrodes used in making the weld contained both cellulose and moisture, which produced hydrogen gas during the welding process. Much of the hydrogen, in atomic form (due to heat of the arc), apparently dissolved in the molten iron. When the weld solidified, solubility for hydrogen decreased. Hydrogen removed from solution was quite free to migrate about in the iron in atomic form. When it reached a void it combined with other atoms of hydrogen to form molecular hydrogen. As this process continued, a tremendous pressure was built up in the void. In many cases this pressure was sufficient to cause extensive cracks to extend from the void.

The material welded in Figure 21 also contained 4.22% silicon; a percentage so high it was prone to fusion-zone cracking. These cracks were extended by the hydrogen gas to the magnitude indicated in the photomicrograph.

With progression into the weld zone at the left in Figure 21, increasing amounts of ferrite existed around the grain boundaries. At the extreme left much ferrite was precipitated out within the austenite grains, forming a Widmänstatten pattern. A considerable carbon pickup was noted, even in the center of the weld.

5. **Annealed structure using E6013 electrodes.** Figure 22 shows a panorama of ductile iron welded in the as-cast condition with E6013 electrodes, and subsequently annealed. In the left of the upper section of the panorama, the parent metal is represented

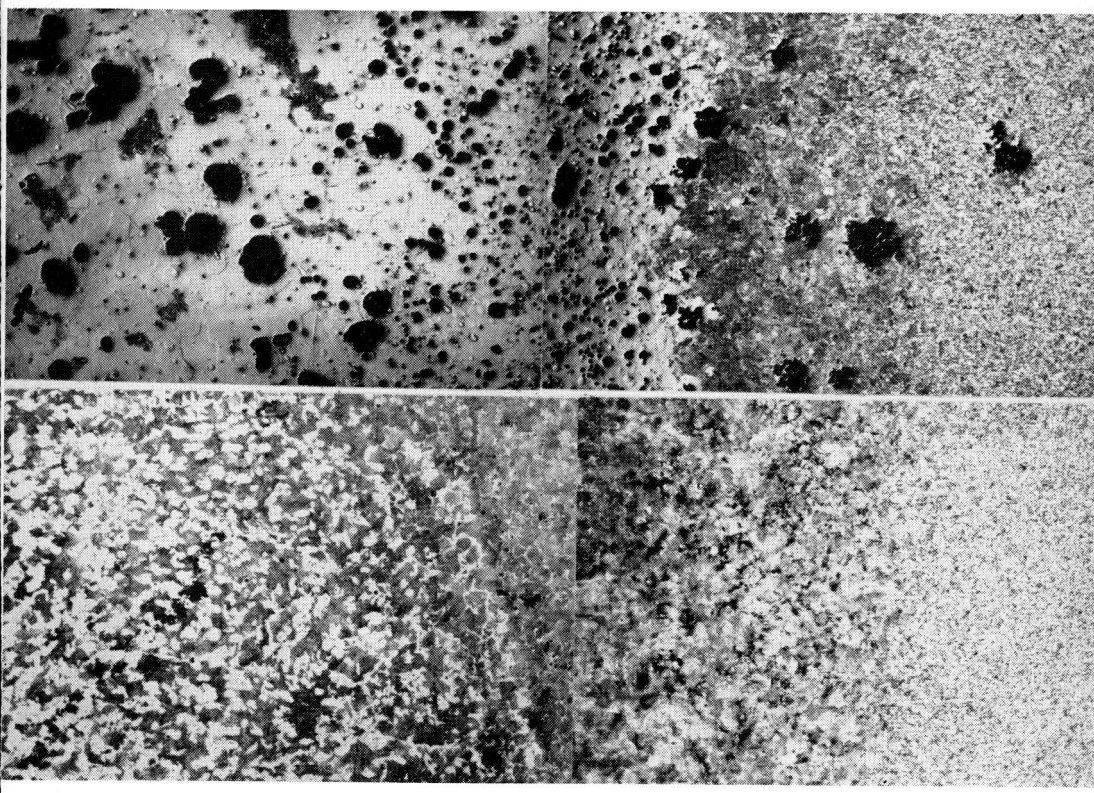

Figure 22. Panorama of ductile iron as welded with E6013 electrodes, after annealing. X100.

where no liquid existed around the nodules. A completely liquid area existed to the right, which formerly consisted of free carbides, martensite, and very fine pearlite; but, after annealing, consisted of a ferrite matrix with nodules of graphite. These nodules, formed well below instead of above the solidus, were very small and placed quite close together. Groups of these small nodules formed a pattern providing a straight line continuity that to some extent lowered the strength and ductility.

The area immediately to the right of the renodulated area (Figure 22), was parent metal in contact with the weld. Carbon transferred from this region to the weld to such an extent an insufficient amount remained to provide renodulization. A hypereutectoid condition then existed, with some free carbides present.

The next region to the right appeared to be very fine-grained (Figure 22). This same region at higher magnification, X500 in Figure 23, shows it had sufficient carbon to be of eutectoid composition. Rapid cooling, effected by the base metal adjoining this region to the left, produced a martensitic, or at least a very fine pearlitic condition. The subsequent anneal produced partial spheroidization of this fine-grained area and massive carbides embedded in a ferrite matrix were noted in coexistence with clearly resolved pearlite.

The area to the left of the partially spheroidized area, in the lower section of Figure 22, was farther into the weld. When this area was examined at X500, it was found to consist of 100% coarse pearlite as a result of the anneal. The fact this region was of eutectoid composition indicated that the region closer to the parent metal was of hypereutectoid composition.

From the fully pearlitic area, progression to the left showed first a ferrite network surrounding pearlite. Farther into the weld, to the left, increasing amounts of ferrite appeared. Magnification of this region to X500 (Figure 24), showed areas of ferrite (white) and pearlite.

The low cost of mild-steel electrodes makes them quite attractive to the consumer. From the foregoing discussion, it is apparent severe problems exist in both the complex structures produced and the content of hydrogen gas that renders their use undesirable. This situation can be somewhat mitigated by the use of low-hydrogen electrodes which do not contain either moisture or organic material in the coating. The gas-forming ingredient of the coating which functions for the exclusion of air from the molten metal, consists of inorganic material. The electrodes are baked at 1100° F. to remove moisture and then sealed in airtight containers. In this condition they are available to the consumer. They should not be exposed to normal atmospheric conditions for more than a few hours prior to use. Nature of the coating is such that higher currents are required during welding, and the integration between weld metal and parent metal is increased accordingly.

6. **Structure of welds with E6015 electrodes.** Deposited weld metal from E6015 low-hydrogen electrodes in an area close to the parent ductile iron which was not preheated is shown in Figure 25. The prior austenite grains were surrounded by a cementite network. They were much larger than the corresponding grains in the deposit from E6013 electrodes because of the higher temperature of application. The carbide network caused fractures of a brittle nature. The Knoop microhardness of this area was 452, whereas the Knoop hardness of a similar portion of the E6013 weld

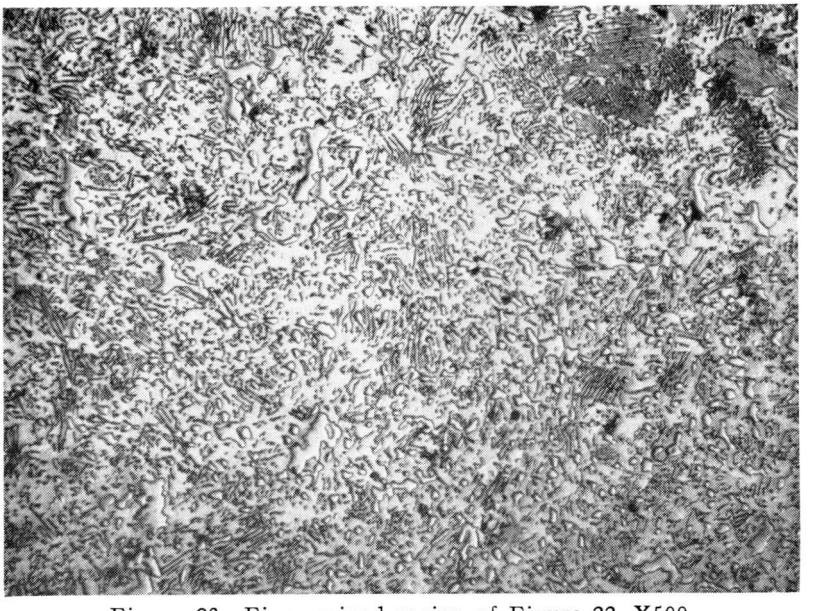

Figure 23. Fine-grained region of Figure 22. X500.

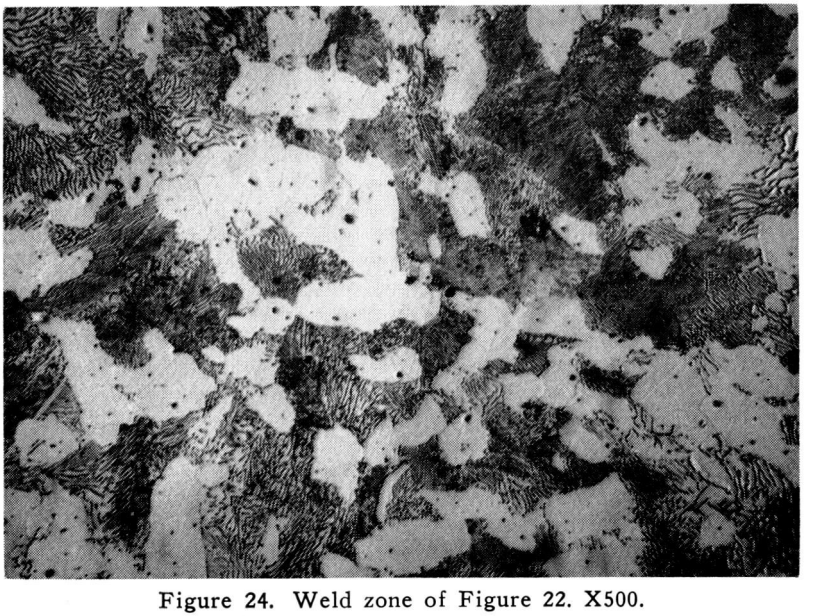

Figure 24. Weld zone of Figure 22. X500.

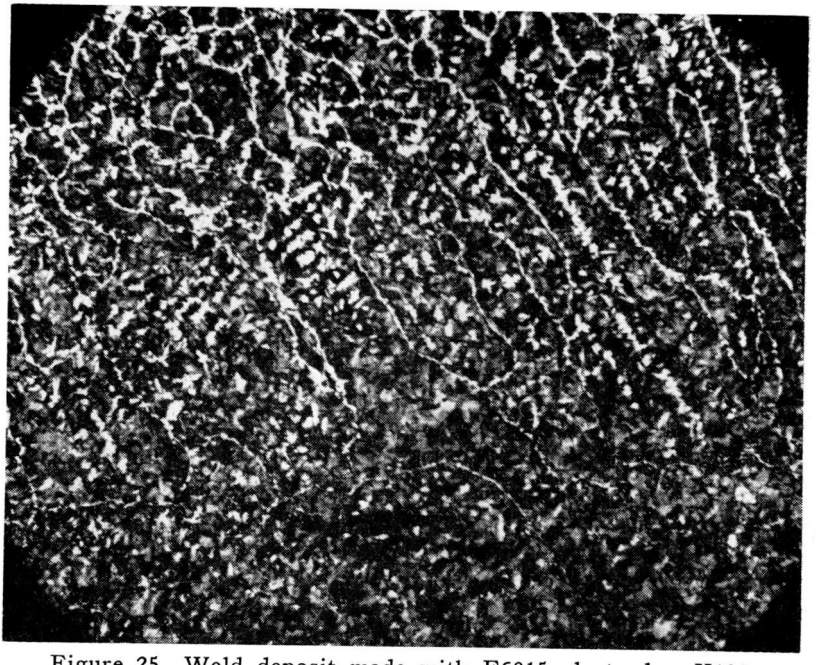

Figure 25. Weld deposit made with E6015 electrodes. X100.

Figure 26. Heat-affected zone of parent metal from weld in Figure 25. X100.

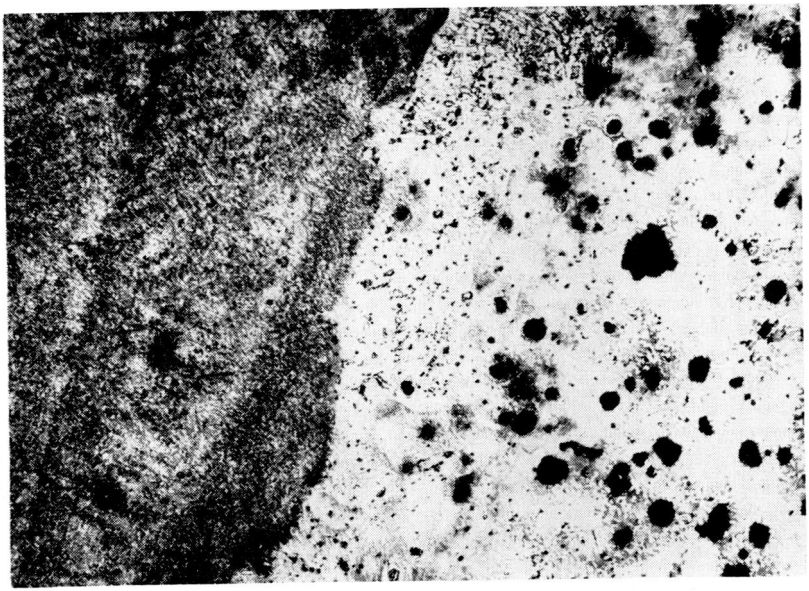

Figure 27. Heat-affected zone of Figure 26 when base metal is preheated. X100.

was 352. Annealing reduced the Knoop hardness of the E6015 weld to 332.

A view of the heat-affected zone of the parent metal, which was very wide, is shown in Figure 26. The heat of welding produced a eutectic condition around the nodules in areas that almost joined. The chilling effect of the base metal, which was not preheated, produced martensite (white) with embedded stringers of carbide (also white) surrounded by an area of very fine, hard pearlite.

When the annealed base metal was preheated to temperatures above 800° F. prior to welding, the heat-affected zone was much narrower (Figure 27). Free carbide stringers still existed, although to a lesser extent, and the exceedingly hard martensite matrix was not in evidence. This was indicative of the beneficial effect of preheating.

Some underbead cracking was found in ductile iron welded in the as-cast condition with low-hydrogen electrodes and followed by annealing (Figure 28). One of the functions of annealing was to degasify the metal. Hydrocarbon gas existing in the as-cast base metal was believed to have been decomposed by the welding arc, producing some atomic hydrogen. This condition, therefore, could be expected when welding the casting prior to annealing. In this

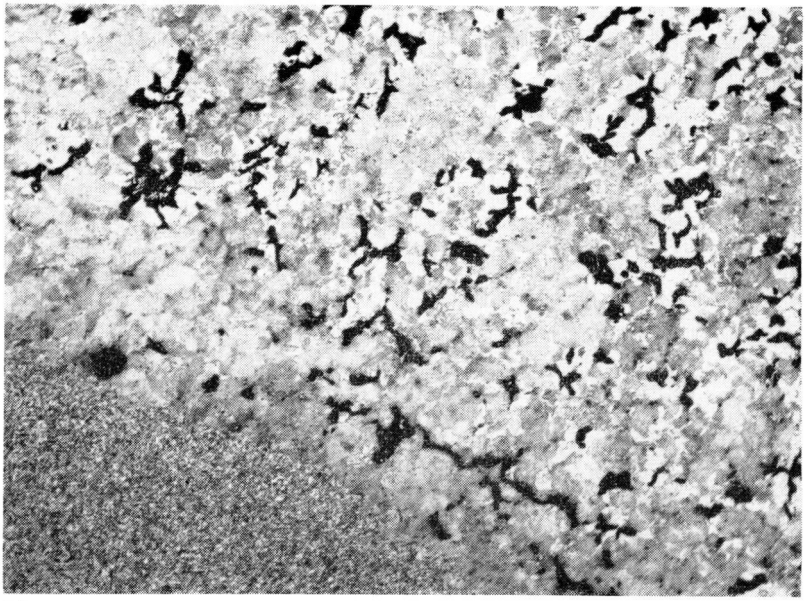

Figure 28. Weld of as-cast ductile iron with E6015 electrodes with subsequent anneal, fusion zone. X100.

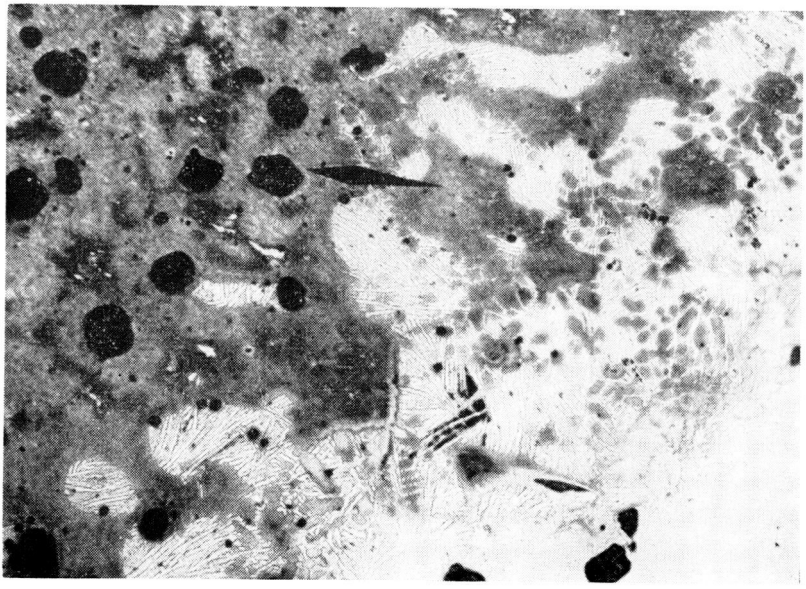

Figure 29. Heat-affected zone, AWS 308-15 electrodes. X100.

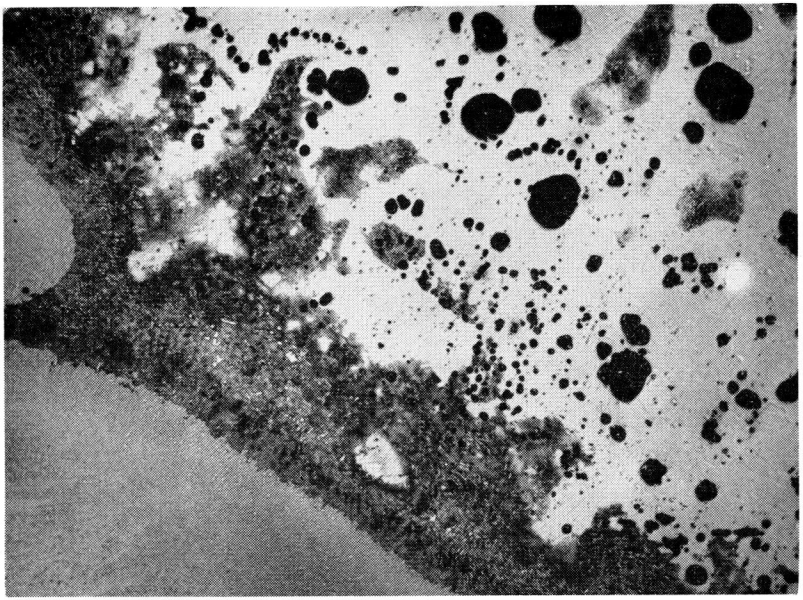

Figure 30. Fusion zone of ductile iron as-cast, welded, then annealed, AWS 308-15 electrodes. X100.

Figure 31. Precipitated carbides in annealed weld with 308-15 electrodes. X100.

case, annealing after welding eliminated both martensite and carbide stringers.

7. **Structure of welds with AWS 308-15 electrodes.** The first austenitic stainless-steel electrodes used were type AWS 308-15, containing 18% chromium and 8% nickel. A very brittle, martensitic heat-affected zone with excess carbide flash resulted, as shown in Figure 29.

When the same electrodes were used on as-cast ductile iron with annealing after welding, the martensite in the fusion zone was converted to a very fine pearlite with some embedded carbides, as shown in Figure 30. This structure was stabilized by chromium carbide. Chromium was evidently imparted to this region of the base metal by the electrode. Carbon that remained in solution in the weld dendrites, due to the fast rate of cooling of the as-welded specimens, was precipitated upon annealing into the dendrite boundaries as chromium carbide. These carbides (Figure 31), formed a very brittle network that resulted in weld failures at low physical values.

8. **Structure of welds with AWS 310-15 electrodes.** Welds were made with stainless-steel electrodes of the AWS 310-15 type, containing 25% chromium and 20% nickel, to determine if any

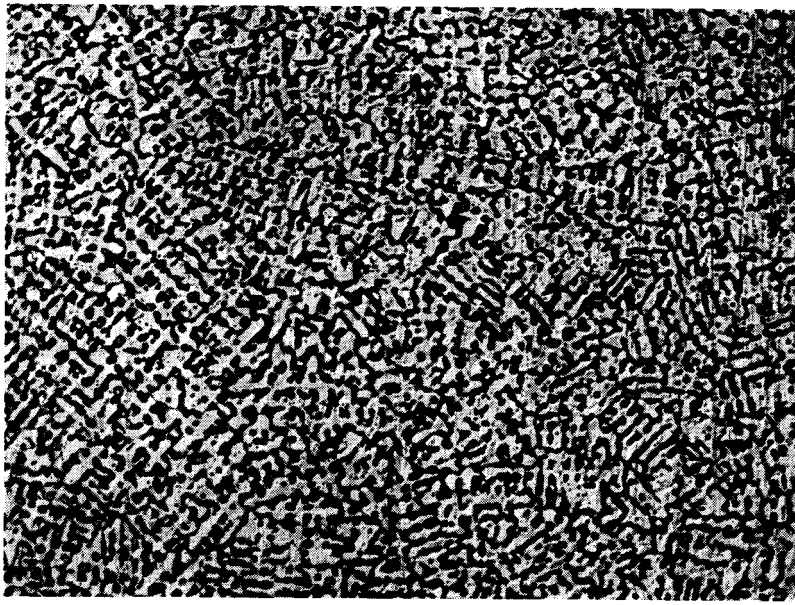

Figure 32. Weld deposit of AWS 308-15 electrodes. X100.

advantages would be derived from the increased alloy content. The austenite dendrites of the weld-metal deposit (Figure 32), were somewhat shorter and wider than those of the type 308 welds. The weld metal was quite soft, with a Knoop hardness of only 142.

The base metal imparted a high-carbon content to these dendrites. Centers of the dendrites, lower in carbon, were first to solidify from the liquid melt. Edges of the dendrites, richer in carbon, solidified last. This specimen was given an electrolytic etch which attacked the high-carbon areas and permitted centers of the dendrites to stand in relief.

A study was made of ductile iron welded in the as-cast condition with type 310 electrodes, and subsequently annealed. The fusion zone showed renodulation in that portion of the base metal altered by the heat of welding. With progression toward the weld area, appreciable amounts of chromium had diffused into the parent metal. The chromium carbides formed were so stable the anneal had very little effect on them. Fine pearlite was stabilized throughout, with many carbide stringers, particularly in the boundaries of prior austenite grains. Carbides also precipitated out into the weld to form a continuous network around the austenite dendrites.

9. **Structure of oxyacetylene welds.** Oxyacetylene fusion welds were made on annealed ductile iron with a filler rod similar to the parent metal. In the as-welded condition the weld metal, upon solidification, consisted of primary austenite dendrites with a substantial network of ledeburite. Upon cooling to below the critical temperature, austenite with embedded nodules was converted into fine pearlite surrounded by a heavy network of cementite (Figure 33). The Knoop hardness of the weld deposit was 432. The sustained high heat of the welding process converted the adjacent parent metal into fine pearlite, with very little ferrite remaining. (See Figure 34.) Although the weld possessed relatively high strength, both it and the adjacent pearlitic parent metal were hard and difficult to machine.

When oxyacetylene welds were annealed, their structures were quite similar to that of the annealed parent metal. Figure 35 shows this condition, with the nodules slightly smaller than those in the base metal. This method of welding was perhaps more promising metallurgically than any other.

10. **Structure of inert gas-shielded arc welds.** Welds made with the inert gas-shielded, tungsten-arc process (as shown in Figure 36) had an appearance in the annealed condition somewhat similar to the oxyacetylene welds. The high temperature involved

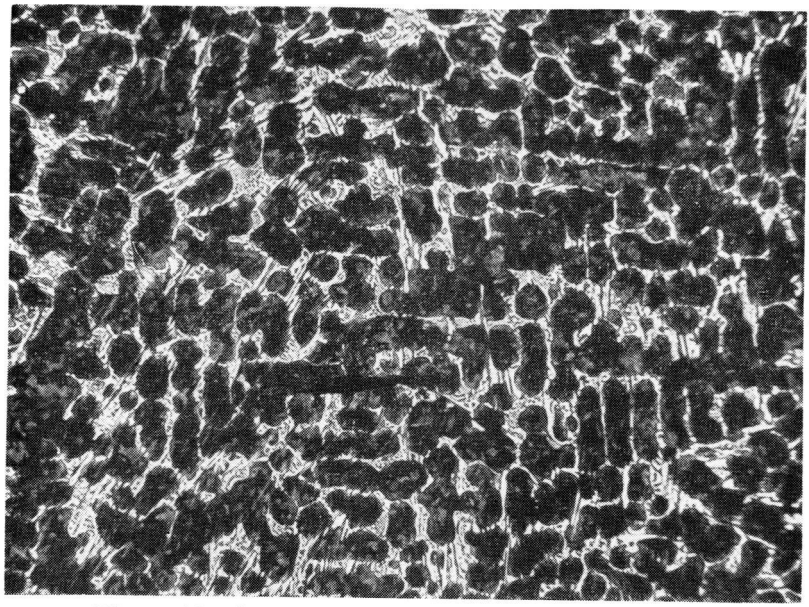

Figure 33. Oxyacetylene weld metal as-welded. X100.

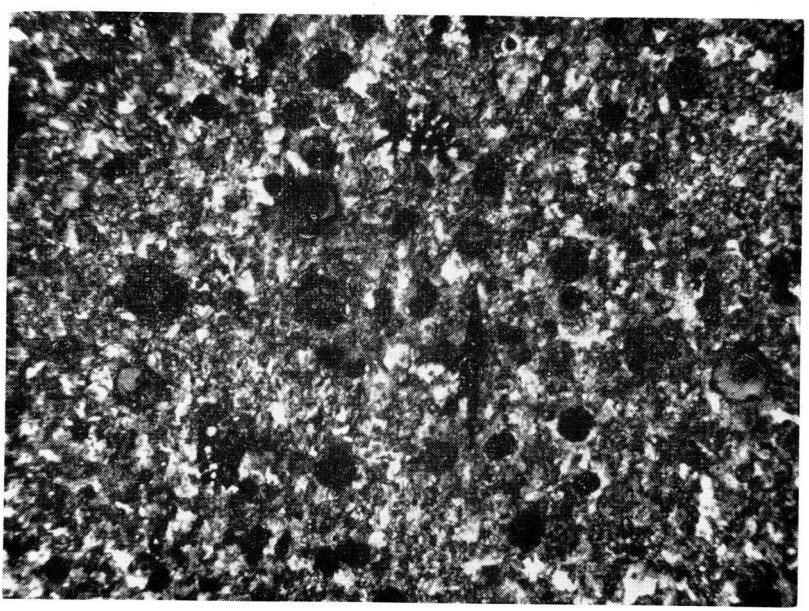

Figure 34. Parent metal heat-affected zone of weld in Figure 33. X100.

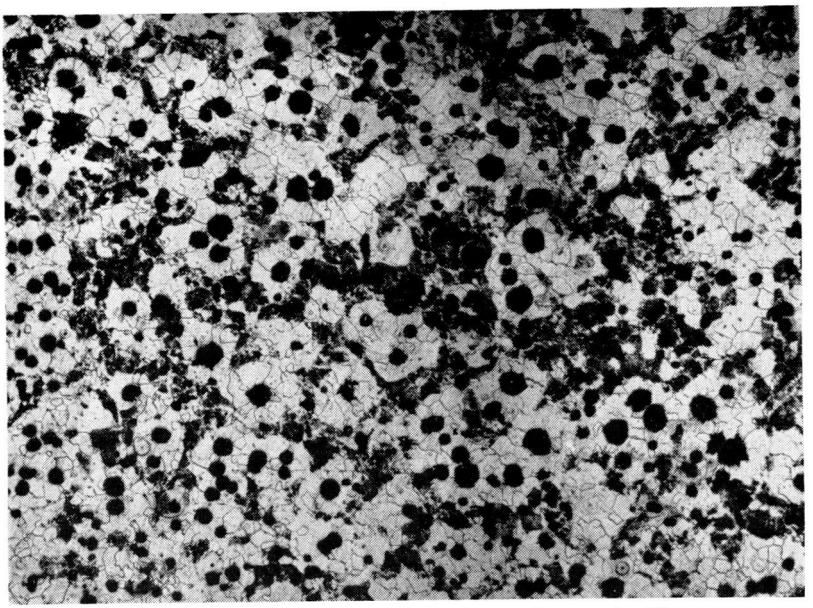

Figure 35. Annealed oxyacetylene-weld metal. X100.

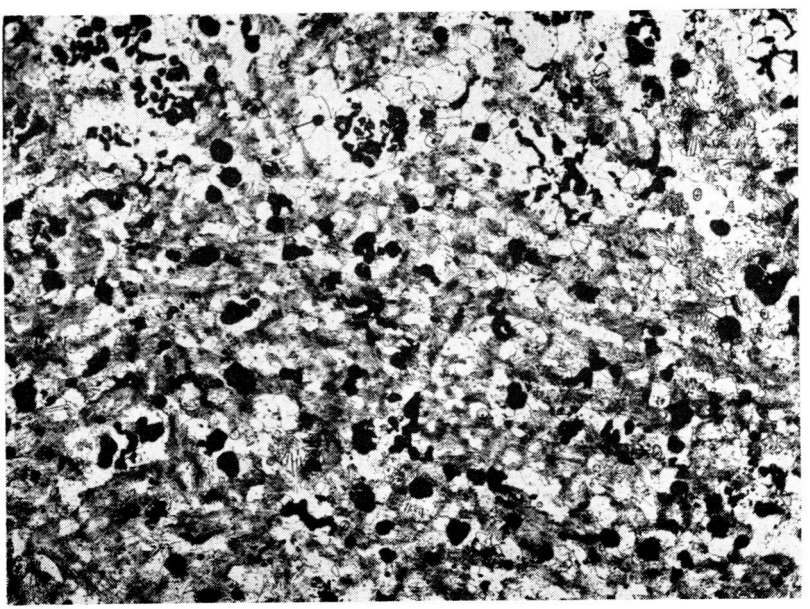

Figure 36. Annealed heliarc-weld deposit. X100.

converted some of the graphite into a quasi-flake form (Figure 37). These semiflake graphitic areas, which tended to exist in the outer layers of the weld, produced lower strength than those of the oxyacetylene welds. Hardness of the annealed weld deposit was about the same as that of the parent metal—Knoop 187.

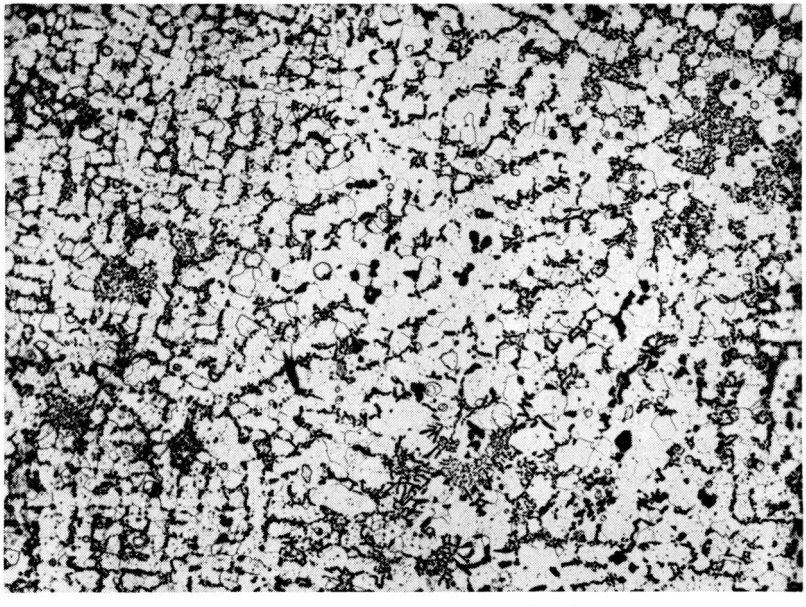

Figure 37. Annealed heliarc-weld deposit in area of partial graphitization. X100.

11. **Structure of carbon-arc welds.** In order to prevent conversion to the semiflake graphite form, lower currents were used for welding with the carbon-arc process than with the heliarc process. The carbon-arc welds had the highest physical values tested, but the nodules of graphite were smaller and spaced closer together than those in the oxyacetylene- or heliarc-welded specimens. This was due to the lower welding current and to the maintenance of a smaller puddle, which resulted in a rapid solidification.

12. **Structure of Ni-Rod 55 welds.** The fusion zone of specimens welded with Ni-Rod 55 nickel-iron electrodes was fairly hard and difficult to machine with tool-steel bits. The fusion zone at the root of the weld was partially martensitic with carbide stringers (Figure 38). When the specimen was annealed after welding, all

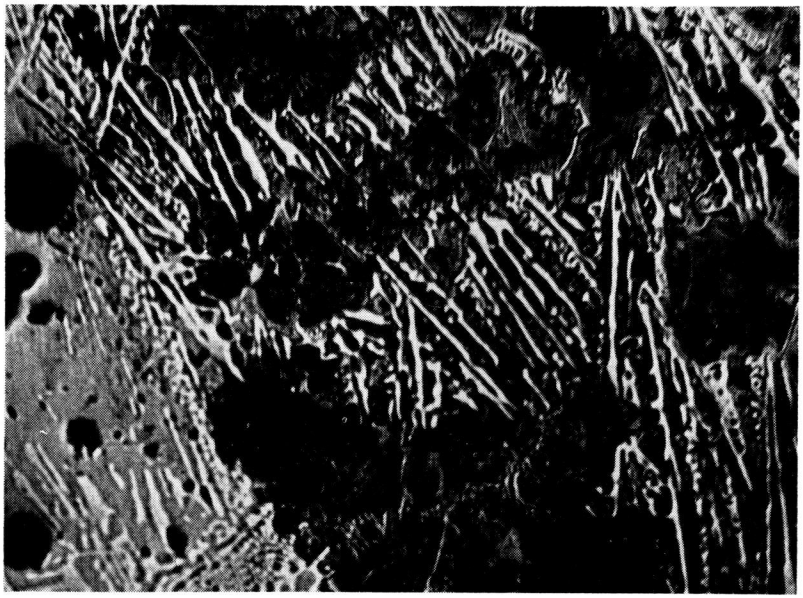

Figure 38. Fusion zone of weld made with Ni-Rod 55. X500.

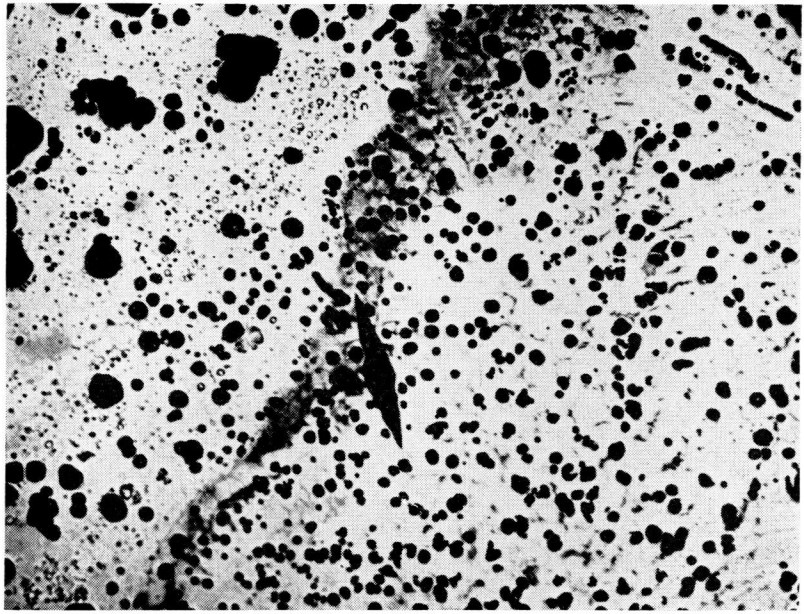

Figure 39. Fusion zone of weld made with Ni-Rod 55 after annealing. X100.

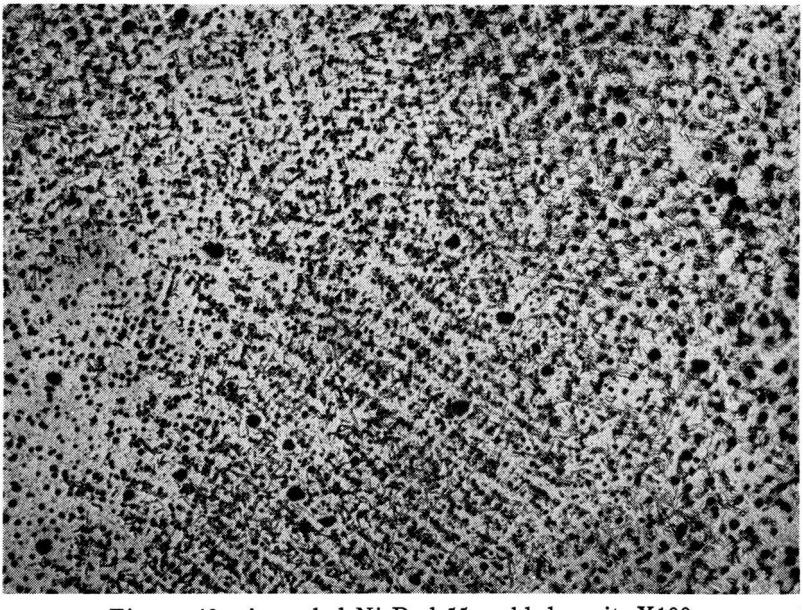

Figure 40. Annealed Ni-Rod 55 weld deposit. X100.

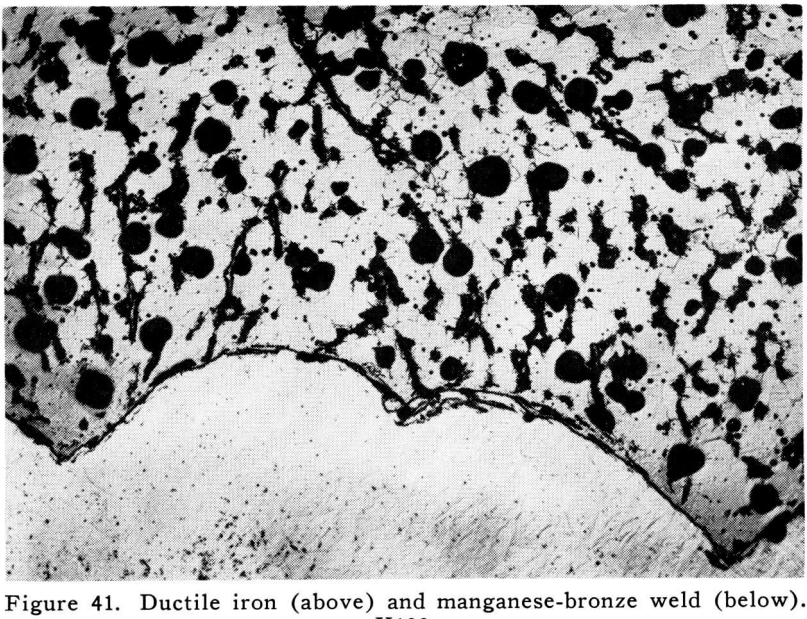

Figure 41. Ductile iron (above) and manganese-bronze weld (below). X100.

trace of martensite and carbide flash was removed, as shown in Figure 39. Primary cored dendrites of weld metal were slightly harder than the parent metal, with a Knoop hardness of 192. These dendrites were somewhat homogenized by annealing (Figure 40).

13. **Structure of bronze welds.** The softest weld deposit was the manganese-bronze (Figure 41), with a Knoop hardness of 108. Structure of the parent metal was not altered by the heat of brazing. It is believed a much more thorough investigation is warranted of this means of joining ductile iron.

VIII. Evaluation of Mechanical Tests

1. **Relationship between mechanical testing and metallography.** A very close correlation exists between mechanical testing and metallography in this study. It is virtually impossible to correctly interpret the reasons for test results without benefit of microscopic examination. On the basis of a metallographic study, quite accurate predictions frequently can be made in regard to the outcome of mechanical tests.

2. **Testing equipment.** A 60,000-pound Southwark-Emery hydraulic testing machine was used in making both the tensile and the flexure tests. All welded specimens were machined to rectangular cross sections for tensile tests, while some parent metal specimens were of rectangular cross sections and others were in the form of 0.505-inch diameter test bars. Preparation of all test bars was described in a previous section.

3. **T-beam flexure test.** The T-beam transverse flexure test bars were loaded by placing them flange down on knife edges on 12-inch centers and exerting a downward force, by means of a third knife edge, on the stem at the centers of the bars. The load required to break these beams ranged from 20,000 pounds to 21,300 pounds, with an average of 20,770 pounds. The average deflection at fracture was 0.485-inch, and the average outer fiber elongation was 4.0% in 2 inches. However, because of the shape of the section being tested, greater elongation should be obtained by means of a standard tensile test.

All of the ductile, cast-iron T-beams had a dark, brittle area of centerline shrinkage in the fracture at the intersection of the leg and the flange. Some cope defects in the nature of drossy, sooty areas also were found in the bottom of the flange. Internal cracking

in defective areas produced lower values than would have been obtained with perfect castings.

Reverse ends of the fractured parent metal T-beam bars were used to produce the composite ductile-iron and mild-steel T-beams. Average load supported by these beams was 18,125 pounds, which represented 88% of the parent metal strength. Although failures were in the weld, this could be expected as the weld itself was at the point of highest applied stress. Center of the fracture was in the fusion zone of the root of the weld, which was identified as a white, carbidic area.

4. **Tensile test of ductile iron welded to steel.** Cast, reduced-section, tensile test bars in the annealed condition produced a maximum ultimate strength of 65,100 psi, a yield strength of 40,000 psi based on a 0.1% offset, and 4.5% elongation in 2 inches. The modulus of elasticity was 23 x 10^6 psi. Other specimens failed at lower values due to centerline shrinkage, slag inclusions, and gas pockets (Figure 42), with 48,500 psi ultimate strength being the lowest recorded value. Although these values compared favorably with those of mild steel, they would have been higher had it not been for defects in the castings.

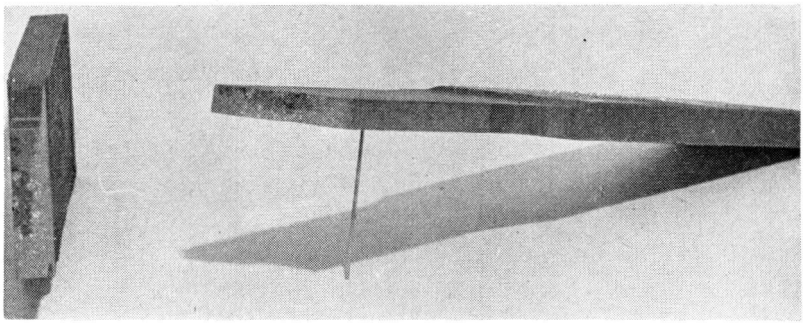

Figure 42. Defects in broken parent metal, reduced-tensile test bar.

The composite ductile-iron and mild-steel test bars produced a maximum ultimate tensile strength of 52,000 psi. Failures were primarily in the weld and carbidic fusion zones, although parent metal failures were obtained. Quality of the castings was such that use of this type was discontinued in favor of Y-block material.

The problem of welding ductile iron to steel is not as complex as that of welding ductile iron to itself. For this reason, subsequent testing was limited only to ductile iron and the more suitable

Y-block castings were produced for this purpose. The Y-block castings produced ultimate tensile strengths of 68,000 psi to 86,000 psi in the as-cast condition, with Rockwell C hardness values of 20 to 25. Ultimate strength values of 55,000 psi to 84,000 psi were obtained for annealed castings, with Rockwell B hardness values from 80 to 90. Values depended upon composition, previously discussed in detail.

5. **Flexure test with rectangular bars.** Parent metal flexure test specimens from 1-inch Y-block material, and also from 1-inch plate material having rectangular cross sections of $1\frac{1}{2}$ inches by $\frac{3}{4}$-inch, were tested on 12-inch centers with third point loading applied to the width. The plate material was not homogenous and fractures with little permanent set occurred during tests. The Y-block material had a yield stress of 23,900 psi in the outer fibers and withstood without fracture a maximum applied load of 6,540 pounds at the maximum bending capacity of the equipment.

Flexure test specimens welded with type 308-15 stainless-steel electrodes failed with deflections of only 0.060 inch to 0.070 inch, and with a maximum applied load of 3,300 pounds. Failures were in the carbidic fusion zone, as shown in Figure 43. The dark areas represented surface fusion-line hot cracks. Rigidity afforded by the first weld passes, which had contracted upon cooling, pre-

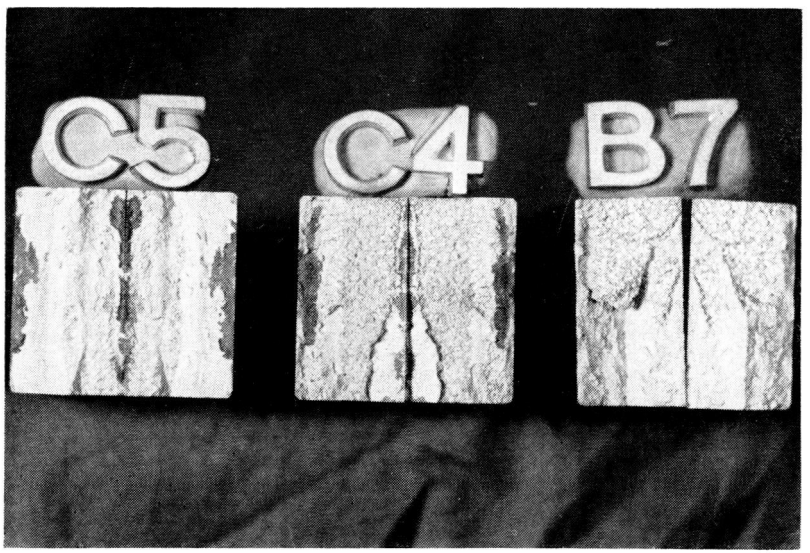

Figure 43. Flexure test bars after fracture.

Figure 44. Flexure test bar (upper) and tensile test bar (lower), before fracture.

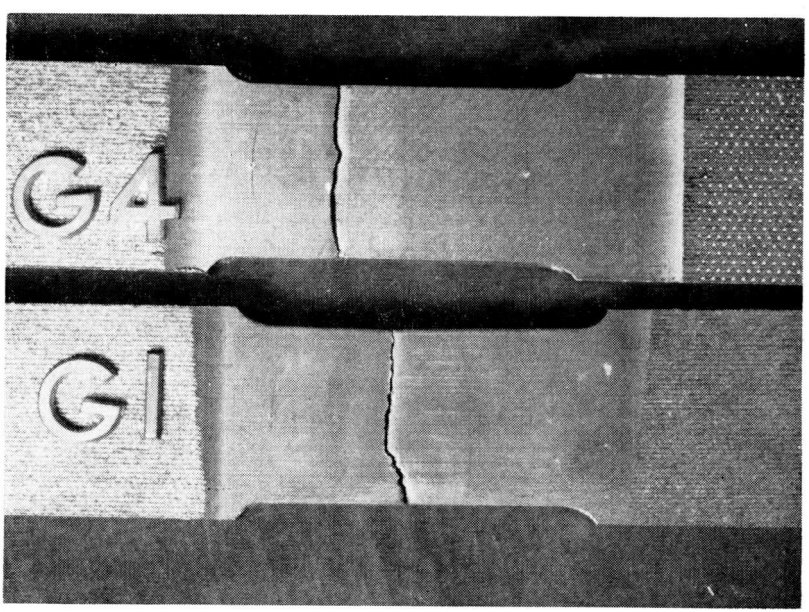

Figure 45. Fractured heliarc-welded test specimens.

vented contraction of the hot, outer weld layers, and the cracks resulted. This condition, not experienced in the thinner sections, could be prevented by maintaining a higher preheat during the entire welding operation.

The surface hot crack can be seen in flexure test specimen C3 prior to the test (Figure 44), and is not present in the thinner tensile test specimen B4.

Because of the poor results obtained, it was decided to discontinue further flexure tests until the tensile testing program was completed so more information would be available regarding the nature of the weldability.

6. **Properties of heliarc welds.** According to results from tensile tests, the most promising methods of welding were fusion processes, using a filler rod of a composition that matched the parent metal. Welds made with the heliarc process produced an average ultimate tensile strength of 36,000 psi for those welded in the as-cast condition followed by annealing, compared with 47,000 psi for those welded after annealing and subsequently reannealed. It was assumed the arc decomposed hydrocarbon gas in the as-cast parent metal during the welding operation and, to a minor extent, provided hydrogen for underbead cracking. These gases were re-

Figure 46. Ends of test bars shown in Figure 45.

moved to such an extent during the annealing operation, this difficulty was not experienced in welding annealed castings. Hardness of the weld, fusion zone, and parent metal was the same—Rockwell B-85.

Examples of heliarc-welded specimens (Figures 45 and 46), show how readily they are machined with high-speed steel milling cutters.

7. **Properties of oxyacetylene welds.** Specimens welded with the oxyacetylene process and parent metal filler rod provided an average ultimate tensile strength of 56,000 psi in the as-welded condition, and 64,000 psi after reannealing. These results are compared with those of the other processes in Figure 47. Because of the experience with heliarc welding, only annealed parent metal was used in making tests. Higher values for reannealed specimens could have been due to higher silicon content in both base metal and filler rod. Impact values of 16.8 ft-lb were obtained for these welds, in comparison with 36.3 ft-lb for the parent metal. Hardness of the weld, fusion zone, and parent metal after annealing was Rockwell B-95, 96, and 90, respectively. Weld and fusion zones of the as-welded material were much harder, with respective values of Rockwell C-34 and C-31.

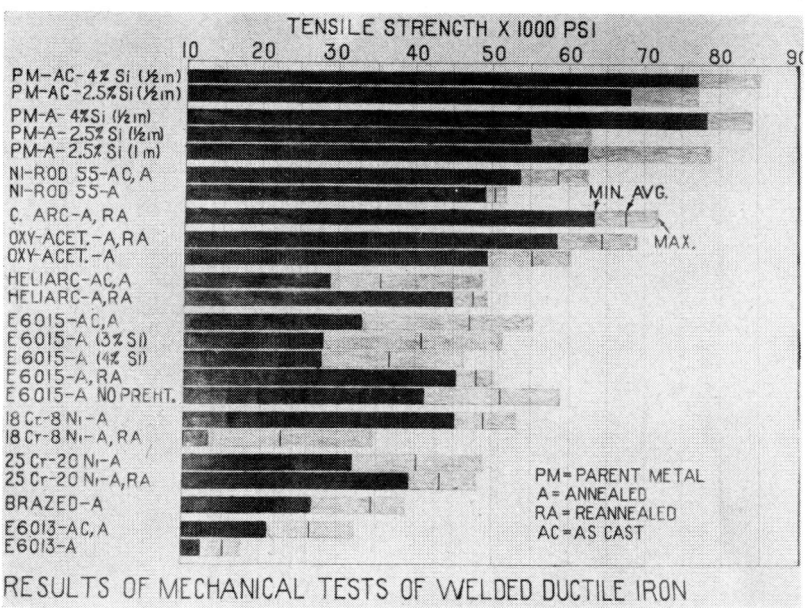

Figure 47. Results of mechanical tests of welded ductile iron.

8. **Properties of carbon-arc welds.** Carbon-arc welded material was of the same composition as the ductile iron that was oxyacetylene welded and reannealed. An average ultimate strength of 67,500 psi with a maximum value of 72,000 psi was the highest obtained with any process. Hardness of the weld and fusion zone was B-95.

Some reversion to quasi-flake graphite during the heliarc-welding process, which was not experienced with oxyacetylene welding, led to the conclusion this resulted from a high temperature in the welding process. As a result, lower current values were used for carbon-arc welding and no graphite reversion was experienced.

9. **Properties of Ni-Rod 55 welds.** The best results obtained with metallic electrodes were with Ni-Rod 55 having a nickel-iron core wire. Failure in the heat-affected zones was experienced with annealed ductile iron welded without preheat. The relatively low ultimate strength of slightly over 50,000 psi was attributed to the high phosphorus content of the base metal. Ductile iron of lower phosphorus content provided an average ultimate tensile strength of 58,000 psi when welded in the as-cast condition and followed by annealing. The hard, narrow fusion zone (Rockwell C-40) of the as-welded material completely disappeared after annealing and had the same hardness as the base metal—Rockwell B-85. Annealing had no effect on hardness of the deposited metal, which was Rockwell B-85 both before and after annealing.

Welds made with Ni-Rod 55 had greater resistance to impact than those made by any other means. Impact resistance of the welds was 28 ft-lb, compared with 36.3 ft-lb for the parent metal.

10. **Properties of welds with E6015 electrodes.** In general, the best results obtained with steel electrodes were with low-hydrogen, mild-steel electrodes of the AWS E6015 type. Ductile iron with increased silicon content did not respond as well to the welding process as that with lower silicon content. Welding of the as-cast material, followed by annealing, was comparable in results with welding of annealed material without reannealing. The highest values obtained were with annealed ductile iron that was not preheated prior to welding.

The ultimate tensile strengths of all low-hydrogen welds ranged between 26,000 psi and 58,000 psi, with a general average of 45,000 psi. Hardness of the fusion zone, Rockwell C-45, was very high in the as-welded condition. After annealing, the fusion zone hardness dropped to Rockwell B-86. Average Rockwell C hardness of 35 to 39 for the as-welded deposited metal dropped to Rockwell C-25 after

annealing. There was a strong tendency toward fusion zone failures in the as-welded condition, and weld failures after annealing. This was attributed to the as-welded, carbidic fusion zone and to the carbide network in the hypereutectoid region of the annealed weld deposits.

11. **Properties of AWS 308-15 welds.** The average ultimate strength value of 48,000 psi for welds with 18-8 stainless-steel electrodes in the as-welded condition was slightly higher than the general average for low-hydrogen, mild-steel weld deposits. This average fell to 23,000 psi when the welds were annealed due to the chromium-carbide network that precipitated in the weld zone.

The weld deposit prior to annealing was relatively soft, Rockwell B-99. The weld was harder after annealing (Rockwell C-48) than the weld or fusion zone of any other process or heat treatment. The hardness of the fusion zone was Rockwell C-30, both before and after annealing. Failures were in the carbidic fusion zone in the as-welded condition and in the weld in the annealed condition.

12. **Properties of AWS 310-15 welds.** Welds with 25-20 stainless-steel electrodes provided lower ultimate strength than those made with low-hydrogen electrodes or with 18-8 stainless electrodes in the annealed condition. All failures were in the fusion zone (Figures 48 and 49), and annealing had little effect on the physical results. Annealed ductile-iron welds in the as-welded condition had an average ultimate strength of 41,000 psi, and those that were re-annealed failed at 43,000 psi. Annealing had very little effect on removing the stable chromium carbides in the fusion zone, but it did reduce the Rockwell C hardness from 35 to 25. A network of chromium carbide resulted from the anneal, but the increase in hardness was very slight—Rockwell C-23 to 26.

13. **Properties of E6013 welds.** Welds with E6013 electrodes were all very poor. A reaction between base metal and electrode coating resulted in entrapped slag in the fusion zone; and also in underbead cracking. Welding was unsatisfactory on both annealed and as-cast material.

Base metal with a high silicon content was much more difficult to weld than that of lower silicon content. The average ultimate strength of the welded low-silicon base metal of 27,000 psi dropped to 16,000 psi when the silicon was increased by 1%. Annealing had no effect on reducing hardness of the deposited weld metal, which was Rockwell C-20 both before and after heat treatment. The fusion zone, with a Rockwell C hardness of 28, was the same hardness as the base metal—Rockwell B-85 after annealing.

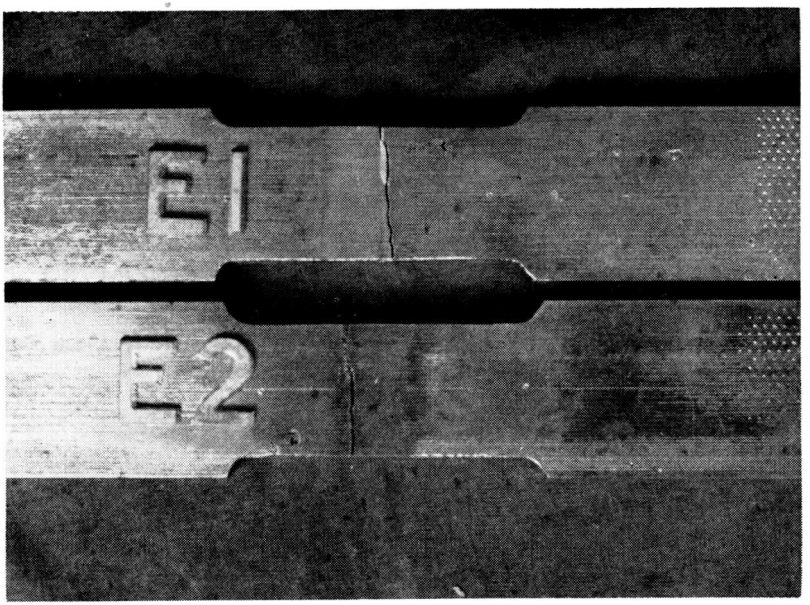

Figure 48. Fusion zone failure of welds made with AWS 310-15 electrodes.

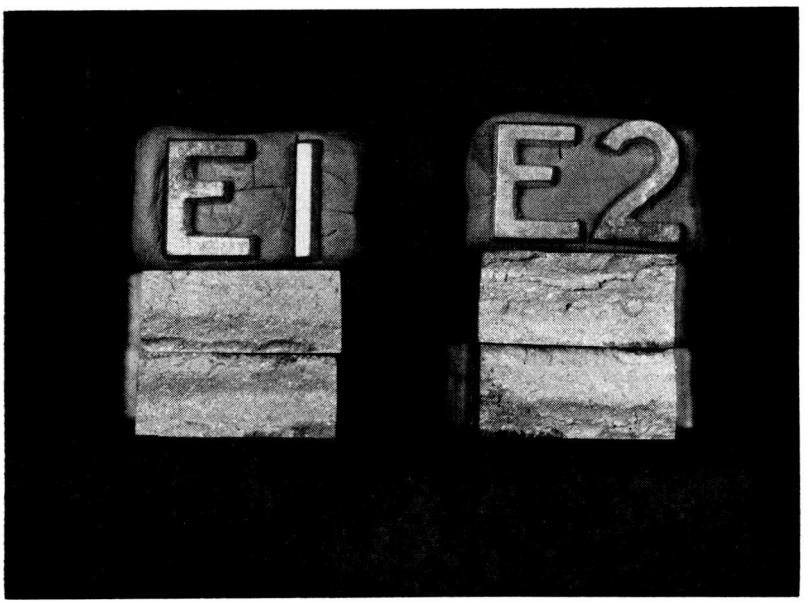

Figure 49. Ends of fractured bars shown in Figure 48.

14. **Properties of bronze welds.** Fractures were in the area of bond between the parent and deposited metal of all bronze-welded specimens. It was felt experimentation with other filler metals, flux, and methods of application (such as the twin carbon arc) would provide an improvement over the average ultimate strength of 34,000 psi obtained during this study.

The manganese-bronze weld deposit was very soft, with a Rockwell B hardness of 65. No heat effect was noted in the bond area between the weld and base metal, which had a hardness value of Rockwell B-88.

15. **Determination of yield.** The stress-strain recorder was used only on annealed parent metal specimens because premature weld failures could damage the equipment. The yield point of welded specimens, observed by a reduction in the rate of applied load, corresponded in general with the yield values obtained for the parent metal.

IX. Recommendations and Conclusions

1. **Scope of the conclusions.** Conclusions derived from results of this investigation are twofold. First, it is evident little information is available and that ductile iron is a sufficiently important material to warrant additional study. The authors are aware that many problems remain to be solved and have included their recommendations in the following paragraph. Second, the authors outline definite practices for welding ductile iron as a result of their studies.

2. **Recommendation for continued investigation.** In regard to the future program of investigation, properties of fusion welding with ductile-iron filler rod appear very good. Oxyacetylene welding is perhaps best from a metallurgical standpoint, even if it is more expensive. The slower cooling rate of the weld deposit of this process in comparison with the carbon arc or inert gas-shielded arc provides larger and fewer carbon nodules. The lower temperature of the deposited metal provides less opportunity for loss of magnesium or silicon, which could cause partial reversion to flake graphite.

One problem is to develop a flux suitable for this method of welding. The effect of adding silicon and magnesium oxide to the flux should be investigated. In general, response to other types of welding in the as-cast condition is poor. In this respect, the oxyacetylene process should be investigated.

The best test results were obtained with carbon-arc welds. The

heliarc-welding process, although more expensive, should be as good as the carbon-arc process. Some silicon or magnesium may be lost during remelting of the ductile-iron filler rod, and the effect of additions of these elements to the weld should be studied.

Subsequent heat treatment is needed to soften the fusion zone of welds made with iron-base electrodes. The cementite network around grain boundaries resulting from a full anneal provides a weak and brittle condition. Heating the weldments for at least an hour at temperatures below the critical is strongly recommended.

Low-hydrogen electrodes produced by different manufacturers should be investigated to determine which is best adapted to ductile iron, as well as the extent to which preheat is required.

Response of the base metal to welding with type 310-15 stainless-steel electrodes was particularly good. Although higher test values were obtained when using low-hydrogen mild steel and type 308-15 stainless-steel electrodes, the type 310-15 stainless-steel electrodes might compare more favorably under certain conditions of heat treatment not included in this investigation. It is recommended that spheroidizing heat treatments be included in any continuation of the work with these electrodes.

The fact no metallurgical changes were noted in the base metal as a result of brazing operations would warrant additional study of this technique.

Using different filler rods, particularly the aluminum bronzes, and different types of flux, should be investigated.

The type of joint and its method of preparation were other variables that could have a pronounced effect on results obtained.

Nonferrous filler rods applied with the double carbon-arc process and alternating current should be investigated.

Some welds were made with aluminum-bronze electrodes which had high strength with good ductility. Due to the high silicon content of the base metal (4.22% Si), failures were consistently in the fusion zone, even after reheating the welds at 1200° F. for 2 hours. An additional study, using these electrodes, should be made upon low-silicon and low-phosphorus base metals.

The microscope is one of the most valuable tools in studying the different techniques mentioned above. Much valuable time will be saved if a careful metallographic study is made prior to conducting time-consuming mechanical tests. A thorough investigation should be made of one process before proceeding to another. The variables of changing composition should be eliminated by obtaining from one heat a sufficient number of castings to conduct a large number of tests.

Mechanical properties other than tensile and hardness should be investigated. Foremost among these are impact, flexure, and fatigue.

Types of welded joints other than butt joints should be included in the study. For example, T-joints of ductile iron to ductile iron, and of other metals to ductile iron, should be included. Tests of assemblies commonly used in fabrication, such as ductile-iron fittings welded to steel tubing, would provide very practical information.

3. **Repair of castings.** It is concluded from results of tests that fusion-welding processes with ductile-iron filler rod provide the most promising means of salvage of defective ductile-iron castings, repair of broken castings, or of welding together simple component castings to produce complicated built-up cast shapes.

Of these processes, the highest rate of production probably can be obtained with the carbon arc or inert gas-shielded arc. The carbon arc is easy to manipulate. It is also the least expensive. The best test results were obtained using the carbon arc. It is recommended that preheats on the order of 1000° F. be used with these fusion processes and that welding be done only on annealed castings. The castings should be reannealed after welding.

The use of Ni-Rod 55 electrodes is recommended for the purposes mentioned in the preceding paragraph if it is desired to eliminate preheating and postheating operations. According to findings in this investigation, these are the only electrodes that can be recommended for use on ductile iron in the as-cast condition. Preheating is desirable for multipass welds and, if possible, postweld heat treatment should be used with these electrodes.

Steel electrodes that contain cellulose or moisture in the coating should not be used under any circumstances for welding ductile iron. Ductile iron that is to be welded should contain less than 0.05% phosphorus and less than 3.5% silicon.

4. **Fabrication of cast weldments.** Metallic electrodes are recommended for integration of ductile iron with wrought steel. The best general choice for this purpose would be Ni-Rod 55 electrodes. If high cost for these electrodes is objectionable, low-hydrogen, mild-steel electrodes are recommended. Some sacrifice of strength and shock resistance may be encountered when using steel electrodes.

If ductile iron is to be welded to stainless steel, AWS type 310-15 electrodes appear to be a good choice. Ni-Rod 55 electrodes also are suitable for this purpose and they would be preferred for welding ductile iron to nonferrous metals. When metallic electrodes

are used, it is recommended postweld heat treatment be given, which would entail heating between 1000° F. and 1200° F. for a period of at least 1 hour.

X. Bibliography

1. Cast metals handbook. American foundrymen's association. 1944.
2. ASTM standards including tentatives, part 1, ferrous metals. American society for testing materials, Baltimore. 1953.
3. Buttner, F. H., H. F. Taylor, and John Wulff. Graphite nodules. American foundryman, 20: 49-50. Oct 1951.
4. DeSy, A. L. Graphite spherulite formation growth. Foundry, 81: 110-114. Nov. 1953.
5. DeSy, A. L. Eliminate second inoculation in new nodular-iron process. American foundryman, 19: 41-45. Feb 1951.
6. Eagan, F. E. and J. D. James. A practical evaluation of ductile cast iron. The iron age, 164: 72-82. Dec 14, 1949.
7. Fishel, W. C. and R. C. Bramlette. Some experiments in preparing nodular iron. American foundryman, 20: 55-56. Sept 1951.
8. Gagnebin, A. P. Ductile iron—its significance to the foundry industry. Foundry, 80: 128-132. June 1952.
9. Gagnebin, A. P., K. D. Mills, and N. D. Pilling. Engineering applications of ductile cast iron. Machine design, 22: 108-114. Jan 1950.
10. Galloway, C. D. Ductile iron for heavy machinery. The iron age, 166: 75-78. Aug 3, 1950.
11. Gries, H. and U. Maushake. On the primary crystallization of spheroidal graphite cast iron. Brutcher's technical translation, Altadena, Calif. (Condensed translation from Giesserei, Technische-Wissenschaflliche, 10:493-502.)
12. Hucke, E. E. and Harry Udin. Welding metallurgy of nodular cast iron. The welding journal, 32: 3785-3855. Aug 1953.
13. Kihlgren, T. E. and H. C. Waugh. Joining of ductile iron by several arc-welding methods. The welding journal, 32: 947-956. Oct 1953.
14. Kraft, R. W. and R. A. Flinn. Interrelation of mechanical properties, casting size, and microstructure of ductile cast iron. Transactions of American society for metals, 44: 282-309. 1952.
15. Mearns, W. C. What you should know about welding ductile iron. The welding engineer, 36: 45-54. Nov 1951.
16. New way to repair ductile iron. Welding engineer, 39: 49. May 1954.
17. Sheley, J. D. Ductile iron replaces alloy gear castings and forgings. Iron age, 167: 99-100. May 10, 1951.
18. Sohn, J., W. Boam, and H. Fisk. Arc welding of ferric and austenitic nodular cast iron. The welding journal, 32: 823-833. Sept 1953.
19. Williamson, C. T. Foundry repair welding. Foundry, 82: 204. Jan 1954.

OREGON STATE COLLEGE
ENGINEERING EXPERIMENT STATION
CORVALLIS, OREGON

LIST OF PUBLICATIONS

Bulletins—

No. 1. Preliminary Report on the Control of Stream Pollution in Oregon, by C. V. Langton and H. S. Rogers. 1929. 15¢.

No. 2 A Sanitary Survey of the Willamette Valley, by H. S. Rogers, C. A. Mockmore, and C. D. Adams. 1930. 40¢.

No. 3 The Properties of Cement-Sawdust Mortars, Plain and with Various Admixtures, by S. H. Graf and R. H. Johnson. 1930. 20¢.

No. 4. Interpretation of Exhaust Gas Analyses, by S. H. Graf, G. W. Gleeson, and W. H. Paul. 1934. 25¢.

No. 5. Boiler-Water Troubles and Treatments with Special Reference to Problems in Western Oregon, by R. E. Summers. 1935. None available.

No. 6. A Sanitary Survey of the Willamette River from Sellwood Bridge to the Columbia by G. W. Gleeson, 1936. 25¢.

No. 7. Industrial and Domestic Wastes of the Willamette Valley, by G. W. Gleeson and F. Merryfield. 1936. 50¢.

No. 8. An Investigation of Some Oregon Sands with a Statistical Study of the Predictive Values of Tests, by C. E. Thomas and S. H. Graf. 1937. 50¢.

No. 9. Preservative Treatments of Fence Posts.
1938 Progress Report on the Post Farm, by T. J. Starker, 1938. 25¢.
Yearly progress reports, 9-A, 9-B, 9-C, 9-D, 9-E, 9-F, 9-G. 15¢.

No. 10. Precipitation-Static Radio Interference Phenomena Originating on Aircraft, by E. C. Starr. 1939. 75¢.

No. 11. Electric Fence Controllers with Special Reference to Equipment Developed for Measuring Their Characteristics, by F. A. Everest. 1939. 40¢.

No. 12. Mathematics of Alignment Chart Construction without the Use of Determinants, by J. R. Griffith. 1940. 25¢.

No. 13. Oil-Tar Cresote for Wood Preservation, by Glenn Voorhies. 1940. 25¢.

No. 14. Optimum Power and Economy Air-Fuel Ratios for Liquefied Petroleum Gases, by W. H. Paul and M. N. Popovich. 1941. 25¢.

No. 15. Rating and Care of Domestic Sawdust Burners, by E. C. Willey. 1941. 25¢.

No. 16. The Improvement of Reversible Dry Kiln Fans, by A. D. Hughes. 1941. 25¢.

No. 17. An Inventory of Sawmill Waste in Oregon, by Glenn Voorhies. 1942. 25¢.

No. 18. The Use of the Fourier Series in the Solution of Beam Problems, by B. F. Ruffner. 1944. 50¢.

No. 19. 1945 Progress Report on Pollution of Oregon Streams, by Fred Merryfield and W. G. Wilmot. 1945. 40¢.

No. 20. The Fishes of the Willamette River System in Relation to Pollution, by R. E. Dimick and Fred Merryfield. 1945. 40¢.

No. 21. The Use of the Fourier Series in the Solution of Beam-Column Problems, by B. F. Ruffner, 1945. 25¢.

No. 22. Industrial and City Wastes, by Fred Merryfield, W. B. Bollen, and F. C. Kachelhoffer. 1947. 40¢.

No. 23. Ten-Year Mortar Strength Tests of Some Oregon Sands, by C. E. Thomas and S. H. Graf. 1948. 25¢.

No. 24. Space Heating by Electric Radiant Panels and by Reverse-Cycle, by Louis Slegel. 1948. 50¢.

No. 25. The Banki Water Turbine, by C. A. Mockmore and Fred Merryfield. Feb 1949. 40¢.

No. 26. Ignition Temperatures of Various Papers, Woods, and Fabrics, by S. H. Graf. Mar 1949. 60¢.

No. 27. Cylinder Head Temperatures in Four Airplanes with Continental A-65 Engines, by S. H. Lowy. July 1949.

No. 28. Dielectric Properties of Douglas Fir at High Frequencies, by J. J. Wittkopf and M. D. Macdonald. July 1949. 40¢.

No. 29. Dielectric Properties of Ponderosa Pine at High Frequencies, by J. J. Wittkopf and M. D. Macdonald. September 1949. 40¢.

No. 30. Expanded Shale Aggregate in Structural Concrete, by D. D. Ritchie and S. H. Graf. Aug 1951. 60¢.

No. 31. Improvements in the Field Distillation of Peppermint Oil, by A. D. Hughes. Aug 1952. 60¢.

No. 32. A Gage for the Measurement of Transient Hydraulic Pressures, by E. F. Rice. Oct 1952. 40¢.

No. 33. The Effect of Fuel Sulfur and Jacket Temperature on Piston Ring Wear as Determined by Radioactive Tracer, by M. Popovich and R. W. Peterson. July 1953. 40¢.

No. 34. Pozzolanic Properties of Several Oregon Pumicites, by C. O. Heath, Jr. and N. R. Brandenburg. 1953. 50¢.

No. 35. Model Studies of Inlet Designs for Pipe Culverts on Steep Grades, by Malcolm H. Karr and Leslie A. Clayton. June 1954. 40¢.

No. 36. A Study of Ductile Iron and Its Response to Welding, by W. R. Rice and O. G. Paasche. Mar 1955. 60¢.

Circulars—

No. 1. A Discussion of the Properties and Economics of Fuels Used in Oregon, by C. E. Thomas and G. D. Keerins. 1929. 25¢.

No. 2. Adjustment of Automotive Carburetors for Economy, by S. H. Graf and G. W. Gleeson. 1930. None available.

No. 3. Elements of Refrigeration for Small Commercial Plants, by W. H. Martin. 1935. None available.

No. 4. Some Engineering Aspects of Locker and Home Cold-Storage Plants, by W. H. Martin. 1938. 25¢.

No. 5. Refrigeration Applications to Certain Oregon Industries, by W. H. Martin. 1940. 25¢.

No. 6. The Use of a Technical Library, by W. E. Jorgensen. 1942. 25¢.

No. 7. Saving Fuel in Oregon Homes, by E. C. Willey. 1942. 25¢.

No. 8. Technical Approach to the Utilization of Wartime Motor Fuels, by W. H. Paul. 1944. 25¢.

No. 9. Electric and Other Types of House Heating Systems, by Louis Slegel. 1946. 25¢.

No. 10. Economics of Personal Airplane Operation, by W. J. Skinner. 1947. 25¢.

No. 11. Digest of Oregon Land Surveying Laws by C. A. Mockmore, M. P. Coopey, B. B. Irving, and E. A. Buckhorn. 1948. 25¢.

No. 12. The Aluminum Industry of the Northwest, by J. Granville Jensen. 1950. None available.

No. 13. Fuel Oil Requirements of Oregon and Southern Washington, by Chester K. Sterrett. 1950. 25¢.

No. 14. Market for Glass Containers in Oregon and Southern Washington, by Chester K. Sterrett. 1951. 25¢.

No. 15. Proceedings of the 1951 Oregon State Conference on Roads and Streets. April 1951. 60¢.

No. 16. Water Works Operators' Manual, by Warren C. Westgarth. March 1953. 75¢.

No. 17. Proceedings of the 1953 Northwest Conference on Road Building. July 1953. 60¢.

Reprints—

No. 1 Methods of Live Line Insulator Testing and Results of Tests with Different Instruments, by F. O. McMillan. Reprinted from 1927 Proc NW Elec Lt and Power Assoc. 25¢.

No. 2. Some Anomalies of Siliceous Matter in Boiler Water Chemistry, by R. E. Summers. Reprinted from Cumbustion, Jan 1935. 10¢.

No. 3. Asphalt Emulsion Treatment Prevents Radio Interference, by F. O. McMillan. Reprinted from Electrical West, Jan 1953. None available.

No. 4. Some Characteristics of A-C Conductor Corona, by F. O. McMillan. Reprinted from Electrical Engineering, Mar 1953. None available.

No. 5. A Radio Interference Measuring Instrument, by F. O. McMillan and H. G. Barnett. Reprinted from Electrical Engineering, Aug 1935. 10¢.

No. 6. Water-Gas Reaction Apparently Controls Engine Exhaust Gas Composition, by G. W. Gleeson and W. H. Paul. Reprinted from National Petroleum News, Feb 1936. None available.

No. 7. Steam Generation by Burning Wood, by R. E. Summers. Reprinted from Heating and Ventilating, Apr 1936. 10¢.

No. 8. The Piezo Electric Engine Indicator, by W. H. Paul and K. R. Eldredge. Reprinted from Oregon State Technical Record, Nov 1935. 10¢.

No. 9. Humidity and Low Temperature, by W. H. Martin and E. C. Willey. Reprinted from Power Plant Engineering, Feb 1937. None available.

No. 10. Heat Transfer Efficiency of Range Units, by W. J. Walsh. Reprinted from Electrical Engineering, Aug 1937. None available.

No. 11. Design of Concrete Mixtures, by I. F. Waterman. Reprinted from Concrete, Nov 1937. None available.

No. 12. Water-Wise Refrigeration, by W. H. Martin and R. E. Summers. Reprinted from Power, July 1938. 10¢.

No. 13. Polarity Limits of the Sphere Gap, by F. O. McMillan. Reprinted from Vol. 58, AIEE Transactions, Mar 1939. 10¢.

No. 14. Influence of Utensils on Heat Transfer, by W. G. Short. Reprinted from Electrical Engineering, Nov 1938. 10¢.

No. 15. Corrosion and Self-Protection of Metals, by R. E. Summers. Reprinted from Industrial Power, Sept and Oct 1938. 10¢.

No. 16. Monocoque Fuselage Circular Ring Analysis, by B. F. Ruffner. Reprinted from Journal of the Aeronautical Sciences, Jan 1939. 10¢.

No. 17. The Photoelastic Method as an Aid in Stress Analysis and Structural Design, by B. F. Ruffner. Reprinted from Aero Digest, Apr 1939. 10¢.

No. 18. Fuel Value of Old-Growth vs. Second-Growth Douglas Fir, by Lee Gabie. Reprinted from The Timberman, June 1939. 10¢.

No. 19. Stoichiometric Calculations of Exhaust Gas, by G. W. Gleeson and F. W. Woodfield, Jr. Reprinted from National Petroleum News, Nov 1939. 10¢.

No. 20. The Application of Feedback to Wide-Band Output Amplifiers, by F. A. Everest and H. R. Johnston. Reprinted from Proc of the Institute of Radio Engineers, Feb 1940. 10¢.

No. 21. Stresses Due to Secondary Bending, by B. F. Ruffner. Reprinted from Proc of First Northwest Photoelasticity Conference, University of Washington, Mar 30, 1940. 10¢.

No. 22. Wall Heat Loss Back of Radiators, by E. C. Willey. Reprinted from Heating and Ventilating, Nov 1940. 10¢.

No. 23. Stress Concentration Factors in Main Members Due to Welded Stiffeners, by W. R. Cherry. Reprinted from The Welding Journal, Research Supplement, Dec 1941. 10¢.

No. 24. Horizontal-Polar-Pattern Tracer for Directional Broadcast Antennas, by F. A. Everest and W. S. Pritchett. Reprinted from Proc of The Institute of Radio Engineers, May 1942. 10¢.

No. 25. Modern Methods of Mine Sampling, by R. K. Meade. Reprinted from The Compass of Sigma Gamma Epsilon, Jan 1942. 10¢.

No. 26. Broadcast Antennas and Arrays. Calculation of Radiation Patterns; Impedance Relationships, by Wilson Pritchett. Reprinted from Communications, Aug and Sept 1944. None available.

No. 27. Heat Losses Through Wetted Walls, by E. C. Willey. Reprinted from ASHVE Journal Section of Heating, Piping, and Air Conditioning, June 1946. 10¢.

No. 28. Electric Power in China, by F. O. McMillan. Reprinted from Electrical Engineering, Jan 1947. 10¢.

No. 29. The Transient Energy Method of Calculating Stability, by P. C. Magnusson. Reprinted from Vol 66, AIEE Transactions, 1947. 10¢.

No. 30. Observations on Arc Discharges at Low Pressures, by M. J. Kofoid. Reprinted from Journal of Applied Physics, Apr 1948. 10¢.

No. 31. Long-Range Planning for Power Supply, by F. O. McMillan. Reprinted from Electrical Engineering, Dec 1948. 10¢.

No. 32. Heat Transfer Coefficients in Beds of Moving Solids, by O. Levenspiel and J. S. Walton. Reprinted from Proc of the Heat Transfer and Fluid Mechanics Institute, 1949. 10¢.

No. 33. Catalytic Dehydrogenation of Ethane by Selective Oxidation, by J. P. McCullough and J. S. Walton. Reprinted from Industrial and Engineering Chemistry, July 1949. 10¢.

No. 34. Diffusion Coefficients of Organic Liquids in Solution from Surface Tension Measurements by R. L. Olson and J. S. Walton. Reprinted from Industrial and Engineering Chemistry, Mar 1951. 10¢.

No. 35. Transients in Coupled Inductance-Capacitance Circuits Analyzed in Terms of a Rolling-Ball Analogue, by P. C. Magnusson. Reprinted from Vol 69, AIEE Transactions, 1950. 10¢.

No. 36. Geometric Mean Distance of Angle-Shaped Conductors, by P. C. Magnusson. Reprinted from Vol 70, AIEE Transactions, 1951. 10¢.

No. 37. Energy—Choose It Wisely Today for Safety Tomorrow, by G. W. Gleeson. Reprinted from ASHVE Journal Section of Heating, Piping, and Air Conditioning, August 1951. 10¢.

No. 38. An Analysis of Conductor Vibration Field Data, by R. F. Steidel, Jr. and M. B. Elton. AIEE Conference Paper presented at Pacific General Meeting, Portland, Oregon, August 23, 1951. 10¢.

No. 39. The Humphreys Constant-Compression Engine, by W. H. Paul and I. B. Humphreys. Reprinted from SAE Quarterly Transactions, April 1952. 10¢.

No. 40. Gas-Solid Film Coefficients of Heat Transfer in Fluidized Coal Beds, by J. S. Walton, R. L. Olson, and Octave Levenspiel. Reprinted from Industrial and Engineering Chemistry, June 1952. 10¢.

No. 41. Restaurant Ventilation, by W. H. Martin. Reprinted from The Sanitarian, Vol 14, No. 6, May-June 1952. 10¢.

No. 42. Electrochemistry in the Pacific Northwest, by Joseph Schulein. Reprinted from the Journal of the Electrochemical Society, June 1953. 20¢.

No. 43. Model Studies of Tapered Inlets for Box Culverts, by Roy H. Shoemaker and Leslie A. Clayton. Reprinted from Research Report 15-B, Highway Research Board, Washington, D. C., 1953. 20¢.

No. 44. Bed-Wall Heat Transfer in Fluidized Systems, by O. Levenspiel and J. S. Walton. Reprints from Heat Transfer-Research Studies, 1954. 10¢.

No. 45. Shunt Capacitors in Large Transmission Networks, by E. C. Starr and E. J. Harrington. Reprinted from Power Apparatus and Systems, Dec 1953. 10¢.

No. 46. The Design and Effectiveness of an Underwater Diffusion Line for the Disposal of Spent Sulphite Liquor, by H. R. Amberg and A. G. Strang. Reprinted from TAPPI, July 1954. 10¢.

No. 47. Compare Your Methods with this Survey, by Arthur L. Roberts and Lyle E. Weatherbee. Reprinted from Western Industry, Dec 1953. 10¢.

THE ENGINEERING EXPERIMENT STATION

Administrative Officers

R. E. KLEINSORGE, President, Oregon State Board of Higher Education.
CHARLES D. BYRNE, Chancellor, Oregon State System of Higher Education.
A. L. STRAND, President, Oregon State College.
G. W. GLEESON, Dean and Director.
D. M. GOODE, Director of Publications.
M. POPOVICH, Assistant Dean.

Station Staff

A. L. ALBERT, Communication Engineering.
H. D. CHRISTENSEN, Aeronautical Engineering.
L. A. CLAYTON, Hydraulic Engineering.
M. P. COOPEY, Highway Engineering.
W. F. ENGESSER, Industrial Engineering.
G. S. FEIKERT, Radio Engineering.
J. B. GRANTHAM, Wood Products.
C. O. HEATH, Engineering Materials.
G. W. HOLCOMB, Civil and Structural Engineering.
A. D. HUGHES, Heat Power and Air Conditioning.
J. G. JENSEN, Industrial Resources.
F. O. McMILLAN, Electrical Engineering.
FRED MERRYFIELD, Sanitary Engineering.
O. G. PAASCHE, Metallurgical Engineering.
W. H. PAUL, Automotive Engineering.
M. C. SHEELY, Manufacturing Processes.
LOUIS SLEGEL, Mechanical Engineering
E. C. STARR, Electrical Engineering.
C. E. THOMAS, Engineering Materials.
J. S. WALTON, Chemical Engineering.

Technical Counselors

R. H. BALDOCK, State Highway Engineer, Salem.
R. R. CLARK, Designing Engineer, Corps of Engineers, Portland District, Portland.
R. W. COWLIN, Director, Pacific Northwest Forest and Range Experiment Station, U. S. Department of Agriculture, Forest Service, Portland.
DAVID DON, Chief Engineer, Public Utilities Commissioner, Salem.
C. M. EVERTS, JR, State Sanitary Engineer, Portland.
PAUL B. McKEE, President, Pacific Power and Light Company, Portland
J. H. POLHEMUS, President, Portland General Electric Company, Portland.
S. C. SCHWARZ, Chemical Engineer, Portland Gas and Coke Company, Portland.
C. K. STERRETT, Manager, Industries Department, Portland Chamber of Commerce.
J. C. STEVENS, Consulting Civil and Hydraulic Engineer, Portland.

Oregon State College

Corvallis

RESIDENT INSTRUCTION

Liberal Arts and Sciences
- Lower Division (Junior Certificate)
- School of Science (B.A., B.S., M.A., M.S., Ph.D. degrees)

Professional Schools
- School of Agriculture (B.S., B.Agr., M.S., M.Agr., Ph.D. degrees)
- School of Business and Technology (B.A., B.S., B.S.S., degrees)
- School of Education (B.A., B.S., Ed.B., M.A., M.S., Ed.M., Ed.D. degrees)
- School of Engineering and Industrial Arts (B.A., B.S., M.A., M.S., A.E., Ch.E., C.E., E.E., I.E., M.E., Min.E., Ph.D. degrees)
- School of Forestry (B.S., B.F., M.S., M.F., F.E. degrees)
- School of Home Economics (B.A., B.S., M.A., M.S., M.H.Ec., Ph.D. degrees)
- School of Pharmacy (B.A., B.S., M.A., M.S., Ph.D. degrees)

Graduate School (M.A., M.S., Ed.M., M.F., M.Agr., M.H.Ec., A.E., Ch.E., C.E., E.E., F.E., I.E., M.E., Min.E., Ed.D., Ph.D. degrees)

Summer Sessions

Short Courses

RESEARCH AND EXPERIMENTATION

General Research

Science Research Institute

Agricultural Experiment Station—
- Central Station, Corvallis
- Union, Moro, Hermiston, Talent, Astoria, Hood River, Pendleton, Medford, and Squaw Butte Branch Stations
- Klamath, Malheur, Red Soils, The Dalles, Central Oregon, and Milton-Freewater Experimental Areas

Engineering Experiment Station

Forest Experiment Station

Oregon Forest Products Laboratory

EXTENSION

Federal Cooperative Extension (Agriculture and Home Economics)

General Extension Division